

PARALLEL MULTILEVEL METHODS FOR SOLVING THE DARCY–FORCHHEIMER MODEL BASED ON A NEARLY SEMICOERCIVE FORMULATION*

JONGHO PARK[†] AND S. MAJID HASSANIZADEH[‡]

Abstract. High-velocity fluid flow through porous media is modeled by prescribing a non-linear relationship between the flow rate and the pressure gradient, called the Darcy–Forchheimer equation. This paper is concerned with the analysis of parallel multilevel methods for solving the Darcy–Forchheimer model. We begin by reformulating the Darcy–Forchheimer model as a nearly semicoercive convex optimization problem via the augmented Lagrangian method. Building on this formulation, we develop a parallel multilevel method, also known as a multilevel additive Schwarz method, within the framework of subspace correction for nearly semicoercive convex problems. The proposed method exhibits robustness with respect to both the nearly semicoercive nature of the problem and the size of the discretized system. To further enhance convergence, we incorporate a backtracking line search scheme and a full approximation scheme. Numerical results validate the theoretical findings and demonstrate the effectiveness and superiority of the proposed approach.

Key words. Darcy–Forchheimer model, Multilevel methods, Subspace correction methods, Nearly semicoercive problems, Augmented Lagrangian method

AMS subject classifications. 65N55, 65N20, 76S05, 90C25

1. Introduction. The Darcy–Forchheimer model characterizes a nonlinear relationship between flow rate and pressure gradient in porous media, and arises in a variety of important applications (see, e.g., [64]). A common situation relates to groundwater flow in high-permeability zones, such as karstic aquifers (see [49]). Also, the flow velocity is high around wellbores in oil and gas reservoirs, in geothermal reservoirs, or in CO₂ sequestration systems, where fluids are extracted or injected (cf. [21]). Another example is in gas reservoirs where high compressibility and velocity make inertial effects important [51, 70]. In some groundwater contamination systems, such as reactive barriers and funnel and gate systems, high groundwater velocity is encountered [29]. Finally, in some manufactured porous media, such as porous catalysts or packed columns, high-speed gas or liquid flows lead to non-Darcy behavior [35, 73]. Various studies have shown that using standard groundwater models based on the Darcy model fail to predict flow fields in systems described above. Often they underestimate velocity by orders of magnitude for a given pressure distribution; see e.g., [39].

Due to its significance, substantial research has been dedicated to developing numerical methods for the Darcy–Forchheimer model. Regarding numerical discretizations, many studies have focused on finite element approaches, which are often classified based on the choice of weak formulation. In [54, 55], mixed finite element methods were developed using a weak formulation with the primal space $H(\operatorname{div}; \Omega) \cap L^3(\Omega)^d$ and the dual space $L^2(\Omega)$, where d denotes the spatial dimension of the domain Ω . In contrast, studies such as [30, 47, 63] adopted a weak formulation with the primal space $L^3(\Omega)^d$ and the dual space $W^{1, \frac{3}{2}}(\Omega)$. For the corresponding discretization,

*This work was conducted while the second author was a visiting professor at KAUST, hosted by the Computer, Electrical and Mathematical Sciences and Engineering Division.

[†]Applied Mathematics and Computational Sciences Program, Computer, Electrical and Mathematical Sciences and Engineering Division, King Abdullah University of Science and Technology (KAUST), Thuwal 23955, Saudi Arabia (jongho.park@kaust.edu.sa).

[‡]Department of Earth Sciences, Utrecht University, 3584, CB, Utrecht, the Netherlands (S.M.Hassanizadeh@uu.nl).

several numerical solvers have been proposed. A Peaceman–Rachford-type iterative method was proposed in [31], while a nonlinear multigrid method for the coupled nonlinear system was developed in [36]. Furthermore, a monolithic multigrid method for coupled problems on fractured domains was introduced in [5]. In [27], a two-level discretization based on a mixed formulation was investigated to reduce the computational cost associated with the nonlinear component. More recently, transformed primal-dual methods with variable preconditioners were studied in [19].

The aim of this paper is to develop efficient numerical methods for the Darcy–Forchheimer model. In particular, we adopt a multilevel approach, building on the well-established philosophy of leveraging hierarchical solvers for nonlinear systems. Multilevel methods are among the most powerful tools for designing numerical solvers in scientific computing and have been extensively studied. Representative works include Bramble–Pasciak–Xu preconditioners [9] and multilevel Schwarz methods [25, 71, 72], in which rigorous convergence theories for multilevel methods were developed. Multilevel methods have also been successfully applied to linear problems involving vector fields; see, e.g., [4, 34]. In addition to the aforementioned studies [5, 36], multilevel techniques have been successfully applied to a wide range of nonlinear problems. The design and analysis of multilevel methods for nonlinear problems remain active areas of research (see, e.g., [13]).

We note that a number of multilevel methods have been proposed for the Darcy–Forchheimer model, or more generally for nonlinear saddle point problems. Although these methods demonstrate excellent numerical performance in practice, theoretical guarantees for fast global convergence remain limited. For example, Newton–Krylov–Schwarz [14, 15] and nonlinear Schwarz preconditioning [16, 17, 24], originally designed for general nonlinear problems, also perform well for the Darcy–Forchheimer model. However, since the nonlinearity is treated by Newton iterations, only fast local convergence can typically be guaranteed; see, e.g., [8].

Some multigrid methods tailored to the Darcy–Forchheimer model were considered in [5, 36]. These works adopt a monolithic multigrid strategy that applies the multilevel approach directly to the nonlinear saddle point formulation, making convergence analysis difficult due to the complexity of the problem. We also note related multigrid methods for other nonlinear saddle point problems, such as the Cahn–Hilliard-type equations [3, 67], where convergence analysis is also unavailable.

Motivated by the above observations, we propose multilevel methods for the Darcy–Forchheimer model whose numerical performance is supported by mathematical analysis. The main idea is to reformulate the Darcy–Forchheimer model as a convex optimization problem using the augmented Lagrangian method [33, 59]. While this strategy was originally proposed for linear problems [44, 45], we extend it here to the nonlinear setting. Once the model is cast into a convex optimization framework, we design parallel multilevel solvers grounded in the theory of subspace correction methods for convex optimization [56, 57, 66], which have been proven effective for a broad class of nonlinear partial differential equations [42, 58]. In particular, the resulting convex optimization problem is nearly semicoercive, i.e., it becomes ill-conditioned as the augmented Lagrangian parameter ϵ tends to zero. To address this challenge, we adopt the recently proposed framework of subspace correction methods tailored to nearly semicoercive convex optimization problems [43].

The main contributions are as follows:

- We show that the coupled nonlinear Darcy–Forchheimer model can be reformulated as a nearly semicoercive convex optimization problem via the augmented Lagrangian approach.

- Based on this formulation, we design efficient parallel multilevel methods with theoretical guarantees.

The remainder of this paper is organized as follows. In [section 2](#), we review finite element discretizations for the Darcy–Forchheimer model. In [section 3](#), we present the reformulation of the Darcy–Forchheimer model as a nearly semicoercive convex optimization problem. In [section 4](#), we propose and analyze relevant parallel multilevel methods. In [section 5](#), we report numerical results that demonstrate the performance of the proposed methods. Finally, in [section 6](#), we provide a summary and conclusions.

2. The Darcy–Forchheimer model. In this section, we briefly review the mathematical formulation of the Darcy–Forchheimer model and its finite element discretization. Relevant references include [\[30, 36, 54\]](#).

2.1. The continuous problem. Let $\Omega \subset \mathbb{R}^d$ be a bounded polyhedral domain with $d = 2, 3$. The steady-state Darcy–Forchheimer model is governed by the following equations. The nonlinear relationship between the Darcy velocity \mathbf{u} and pressure p [\[32\]](#) is given by

$$(2.1a) \quad \frac{\mu}{\rho} \mathbf{K}^{-1} \mathbf{u} + \frac{\beta}{\rho} |\mathbf{u}| \mathbf{u} + \nabla p = \mathbf{f} \quad \text{in } \Omega,$$

where \mathbf{K} is the permeability tensor, ρ is the fluid density, μ is the fluid viscosity, β is the Forchheimer coefficient, and \mathbf{f} is the external body force per unit volume.

The conservation of mass is expressed as

$$(2.1b) \quad \operatorname{div} \mathbf{u} = g \quad \text{in } \Omega,$$

where g is a prescribed source or sink term representing mass production or depletion.

For the boundary condition, for clarity and simplicity, we consider the case of a pure homogeneous Dirichlet boundary condition:

$$(2.1c) \quad p = 0 \quad \text{on } \partial\Omega.$$

2.2. Finite element approximations. Various finite element approximations have been proposed in the literature for approximating the Darcy–Forchheimer model [\[30, 47, 54, 55, 63\]](#); see also [\[36\]](#) and the references therein. Among these, we adopt the approach introduced in [\[54\]](#), which employs Raviart–Thomas-type finite element discretizations [\[7\]](#).

We define the function spaces

$$\begin{aligned} X &= \{ \mathbf{v} \in L^3(\Omega)^d : \operatorname{div} \mathbf{v} \in L^2(\Omega) \}, \\ M &= L^2(\Omega). \end{aligned}$$

Observe that X is the intersection of two Banach spaces, $H(\operatorname{div}; \Omega)$ and $L^3(\Omega)^d$:

$$X = H(\operatorname{div}; \Omega) \cap L^3(\Omega)^d.$$

Equipped with the norm

$$\|\mathbf{v}\|_X = \left(\|\operatorname{div} \mathbf{v}\|_{L^2(\Omega)}^2 + \|\mathbf{v}\|_{L^2(\Omega)}^2 + \|\mathbf{v}\|_{L^3(\Omega)}^2 \right)^{1/2},$$

the space X becomes a uniformly smooth and uniformly convex Banach space (cf. [\[50\]](#)).

The weak formulation of (2.1) defined on (X, M) is as follows: find $(\mathbf{u}, p) \in X \times M$ such that

$$(2.2) \quad \begin{aligned} \frac{\mu}{\rho} \int_{\Omega} \mathbf{K}^{-1} \mathbf{u} \cdot \mathbf{v} \, dx + \frac{\beta}{\rho} \int_{\Omega} |\mathbf{u}| \mathbf{u} \cdot \mathbf{v} \, dx - \int_{\Omega} p \operatorname{div} \mathbf{v} \, dx &= \int_{\Omega} \mathbf{f} \cdot \mathbf{v} \, dx \quad \forall \mathbf{v} \in X, \\ \int_{\Omega} q \operatorname{div} \mathbf{u} \, dx &= \int_{\Omega} g q \, dx \quad \forall q \in M. \end{aligned}$$

Let \mathcal{T}_h be a quasi-uniform partition of Ω into finite elements, where h denotes the characteristic mesh size. Let $X_h \times M_h \subset X \times M$ be a Raviart–Thomas-type conforming mixed finite element space [7] defined on \mathcal{T}_h . For example, in two dimensions ($d = 2$), if each element $T \in \mathcal{T}_h$ is a rectangle, the local spaces X_h and M_h on T are defined as

$$(2.3) \quad X_h(T) := Q_{k+1,k}(T) \oplus Q_{k,k+1}(T), \quad M_h(T) := Q_{k,k}(T),$$

for $k \geq 0$, where $Q_{k,\ell}(T)$ denotes the set of polynomials on T of degree at most k and ℓ in each coordinate direction, respectively. Additional examples of Raviart–Thomas-type conforming mixed finite element spaces can be found in [54, Table 1].

The finite element formulation of (2.2) using the discrete space $X_h \times M_h$ is given as follows: find $(\mathbf{u}_h, p_h) \in X_h \times M_h$ such that

$$(2.4) \quad \begin{aligned} \frac{\mu}{\rho} \int_{\Omega} \mathbf{K}^{-1} \mathbf{u}_h \cdot \mathbf{v} \, dx + \frac{\beta}{\rho} \int_{\Omega} |\mathbf{u}_h| \mathbf{u}_h \cdot \mathbf{v} \, dx - \int_{\Omega} p_h \operatorname{div} \mathbf{v} \, dx &= \int_{\Omega} \mathbf{f} \cdot \mathbf{v} \, dx \quad \forall \mathbf{v} \in X_h, \\ \int_{\Omega} q \operatorname{div} \mathbf{u}_h \, dx &= \int_{\Omega} g q \, dx \quad \forall q \in M_h. \end{aligned}$$

Existence and uniqueness results for (2.4) can be found in [54, Theorem 3.5].

We define the functional $F: X \rightarrow \mathbb{R}$ by

$$(2.5) \quad F(\mathbf{v}) = \frac{\mu}{2\rho} \int_{\Omega} \mathbf{K}^{-1} \mathbf{v} \cdot \mathbf{v} \, dx + \frac{\beta}{3\rho} \int_{\Omega} |\mathbf{v}|^3 \, dx - \int_{\Omega} \mathbf{f} \cdot \mathbf{v} \, dx, \quad \mathbf{v} \in X.$$

One readily observes that (2.4) corresponds to the optimality condition of the following saddle-point problem:

$$(2.6) \quad \min_{\mathbf{v} \in X_h} \max_{q \in M_h} \left\{ F(\mathbf{v}) - \int_{\Omega} q (\operatorname{div} \mathbf{v} - g) \, dx \right\}.$$

By invoking Fenchel–Rockafellar duality [37, 60], the saddle-point problem (2.6) is equivalent to a constrained convex optimization problem. Namely, (2.4) can be reformulated as a constrained minimization problem, as summarized in Proposition 2.1.

PROPOSITION 2.1. *The function $\mathbf{u}_h \in X_h$ is a primal solution of (2.4) if and only if it solves the following convex optimization problem with a linear constraint:*

$$(2.7) \quad \min_{\mathbf{v} \in X_h} F(\mathbf{v}) \quad \text{subject to} \quad \operatorname{div} \mathbf{v} = g_h,$$

where the functional F is defined in (2.5), and g_h is the $L^2(\Omega)$ -orthogonal projection of g onto M_h .

3. Reduction to a nearly semicoercive convex optimization problem.

In this section, we show that the finite element discretization (2.4) can be reduced to a nearly semicoercive convex optimization problem if we proceed similarly as in [45, Section 2.2]. More precisely, we show that an iteration of the augmented Lagrangian method [33, 59] for solving the constrained optimization problem (2.7) is equivalent to a nearly semicoercive convex optimization problem [43], where the convergence rate of the augmented Lagrangian method can be arbitrarily fast.

The augmented Lagrangian method [33, 59] for solving (2.7) is summarized in Algorithm 3.1.

Algorithm 3.1 Augmented Lagrangian method for solving (2.7)

Given $\epsilon > 0$:

Choose $p_h^{(0)} \in M_h$.

for $n = 0, 1, 2, \dots$ **do**

$$\mathbf{u}_h^{(n+1)} = \arg \min_{\mathbf{v} \in X_h} \left\{ F(\mathbf{v}) - \int_{\Omega} p_h^{(n)} \operatorname{div} \mathbf{v} \, dx + \frac{1}{2\epsilon} \int_{\Omega} (\operatorname{div} \mathbf{v} - g_h)^2 \, dx \right\}$$

$$p_h^{(n+1)} = p_h^{(n)} - \epsilon^{-1} (\operatorname{div} \mathbf{u}_h^{(n+1)} - g_h)$$

end for

In the linear case, for instance when $\beta = 0$ in (2.4), it was shown in [45, Lemma 2.1] that the augmented Lagrangian method can achieve arbitrarily fast convergence by choosing ϵ sufficiently small; similar results can also be found in [40, 41]. In Theorem 3.1, we show that this property remains valid in the nonlinear case. In Theorem 3.1, D_F^{sym} denotes the *symmetrized Bregman divergence* associated with F [1, 53], defined by

$$(3.1) \quad D_F^{\text{sym}}(v, w) = \langle F'(v) - F'(w), v - w \rangle, \quad v, w \in V,$$

where $F'(v) \in V^*$ denotes the Gâteaux derivative of F at v , and $\langle \cdot, \cdot \rangle: V^* \times V \rightarrow \mathbb{R}$ denotes the duality pairing on V . We also note that the augmented Lagrangian method in a general abstract setting is analyzed in section A.

THEOREM 3.1. *Let $\{(\mathbf{u}_h^{(n)}, p_h^{(n)})\}$ be the sequence generated by the augmented Lagrangian method presented in Algorithm 3.1. Then, there exists a constant $\mu > 0$, independent of ϵ , such that*

$$D_F^{\text{sym}}(\mathbf{u}_h^{(n+1)}, \mathbf{u}_h) \leq \frac{\epsilon}{4} \|p_h^{(n)} - p_h\|_{L^2(\Omega)}^2 \leq \frac{\epsilon}{4} \left(\frac{\epsilon}{\mu + \epsilon} \right)^{2n} \|p_h^{(0)} - p_h\|_{L^2(\Omega)}^2, \quad n \geq 0,$$

where the symmetrized Bregman divergence D_F^{sym} is defined in (3.1).

Proof. Thanks to (A.2), Theorem A.3, and Theorem A.4, it suffices to verify that $F^* \circ \operatorname{div}^*$ is locally strongly convex on M_h , where $F^*: X_h \rightarrow \mathbb{R}$ is the Legendre–Fenchel conjugate of F defined in (A.4), and $\operatorname{div}^*: M_h \rightarrow X_h$ denotes the $L^2(\Omega)$ -adjoint of $\operatorname{div}: X_h \rightarrow M_h$. Since F is locally smooth on X_h (see section 4.2), it follows from [31] that F^* is locally strongly convex. Moreover, because div^* is injective, the composition $F^* \circ \operatorname{div}^*$ inherits local strong convexity. This completes the proof. \square

Remark 3.2. Since Theorem 3.1 shows that smaller ϵ yields faster convergence of Algorithm 3.1, it may be desirable to choose ϵ as small as possible. However, in practice, choosing ϵ too small may lead to numerical instability, which should be avoided for robust computation. Fortunately, we will observe in section 5 that ϵ need

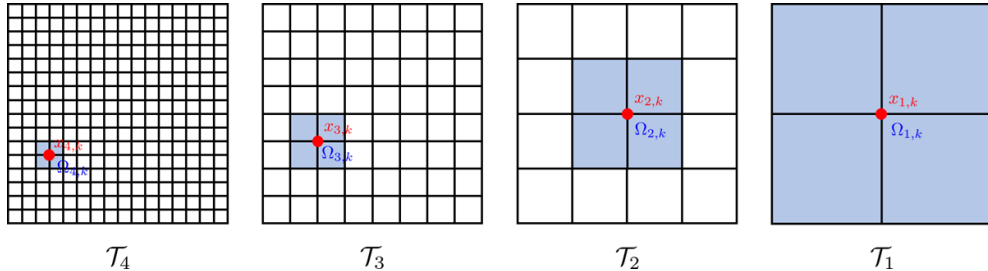


FIG. 1. Multilevel mesh hierarchy $\{\mathcal{T}_j\}_{j=1}^J$ for a rectangular grid \mathcal{T}_h ($J = 4$). For each vertex $x_{j,k}$ of the mesh \mathcal{T}_j (depicted in red), the blue region represents the corresponding subdomain $\Omega_{j,k}$.

not be too small; heuristically, values ranging from 10^{-3} to 10^{-1} are sufficient for fast convergence. Relevant discussions for the linear case can be found in, e.g., [41].

Theorem 3.1 implies that the convergence rate of the augmented Lagrangian method for solving (2.7) can be made arbitrarily fast by choosing ϵ sufficiently small. In other words, the number of iterations required to achieve a prescribed level of accuracy becomes very small as ϵ decreases. Relevant numerical results illustrating this behavior will be provided in section 5.

In this sense, the mixed formulation (2.4) can be viewed as being reduced to a convex optimization problem of the form

$$(3.2) \quad \min_{\mathbf{v} \in X_h} \left\{ F^\epsilon(\mathbf{v}; q_h) := \frac{1}{2} \int_{\Omega} (\operatorname{div} \mathbf{v} - q_h)^2 dx + \epsilon \left[F(\mathbf{v}) - \int_{\Omega} q_h \operatorname{div} \mathbf{v} dx \right] \right\}$$

for some $q_h \in M_h$. When there is no ambiguity, we simply write $F^\epsilon(\mathbf{v}) = F^\epsilon(\mathbf{v}; q_h)$. In what follows, it suffices to focus on solving (3.2). We denote the solution of (3.2) by $\mathbf{u}_h^\epsilon \in X_h$.

A major difficulty in solving (3.2) numerically is that the problem is nearly semi-coercive [43] (cf. nearly singular in the linear case [45]) due to the nontrivial kernel of div . As a result, (3.2) becomes increasingly ill-conditioned as ϵ becomes small, causing conventional iterative solvers to converge very slowly.

In the following section, we present the construction of an efficient iterative solver for (3.2) that remains robust with respect to both small ϵ and the mesh size h .

4. Multilevel methods. In this section, we propose a multilevel method for solving the nearly semicoercive convex optimization problem (3.2) that is robust with respect to both the augmented Lagrangian parameter ϵ and the mesh size h . Building upon the abstract theory of subspace correction methods for solving nearly semicoercive convex optimization problems developed in [43], we construct a patch-based multilevel method with Schwarz smoothers, similarly as in [4, 44]. We also present a backtracking strategy for line search in the multilevel method [57], which makes the algorithm more practical in the sense that it is even faster and does not require a predetermined step size.

4.1. Multilevel subspace correction. We assume that the partition \mathcal{T}_h is part of a nested sequence of quasi-uniform partitions $\{\mathcal{T}_j\}_{j=1}^J$, where $\mathcal{T}_h = \mathcal{T}_J$ and each \mathcal{T}_j , $1 \leq j \leq J$, has a characteristic element size h_j . The quasi-uniformity constants are independent of j , and the mesh sizes satisfy $h_j \approx \gamma^j$ for some coarsening factor $\gamma \in (0, 1)$. See Figure 1 for an example of a rectangular grid \mathcal{T}_h when $J = 4$.

For each \mathcal{T}_j , we define the finite element space V_j , of the same type as $V := X_h$. It follows that

$$V_1 \subset V_2 \subset \dots \subset V_J = V.$$

Let \mathcal{V}_j be the set of all internal vertices of \mathcal{T}_j , and let $n_j = |\mathcal{V}_j|$. For each $x_{j,k} \in \mathcal{V}_j$, $1 \leq k \leq n_j$, we define

$$\Omega_{j,k} = \bigcup \{ \tau \in \mathcal{T}_j : x_{j,k} \in \partial\tau \}.$$

We define the subspace $V_{j,k}$ as

$$V_{j,k} = \{ v \in V_j : \text{supp } v \subset \bar{\Omega}_{j,k} \},$$

so that we have

$$V_j = \sum_{k=1}^{n_j} V_{j,k}.$$

Then we have the following vertex-based multilevel space decomposition of V :

$$(4.1) \quad V = \sum_{j=1}^J \sum_{k=1}^{n_j} V_{j,k}.$$

Such vertex-based space decomposition for vector field problems was previously considered in, e.g., [4, 44].

Now, we are ready to present our proposed multilevel method. The proposed method is a parallel subspace correction method [43, 56, 66] for solving (3.2) based on the multilevel space decomposition (4.1), as summarized in [Algorithm 4.1](#).

Algorithm 4.1 Parallel multilevel method for solving (3.2)

Given $\tau > 0$:

Choose $\mathbf{u}^{(0)} \in V$.

for $n = 0, 1, 2, \dots$ **do**

for $j = 1, 2, \dots, J$ **do**

for $k = 1, 2, \dots, n_j$ **do**

$$\mathbf{w}_{j,k}^{(n+1)} = \arg \min_{\mathbf{w}_{j,k} \in V_{j,k}} F^\epsilon(\mathbf{u}^{(n)} + \mathbf{w}_{j,k})$$

end for

end for

$$\mathbf{u}^{(n+1)} = \mathbf{u}^{(n)} + \tau \sum_{j=1}^J \sum_{k=1}^{n_j} \mathbf{w}_{j,k}^{(n+1)}$$

end for

Note that each $\mathbf{w}_{j,k}^{(n+1)}$ -local problem in [Algorithm 4.1](#) is a convex optimization problem of small dimension, which can be solved robustly and efficiently using second-order optimization algorithms, such as the damped Newton method [8]. Moreover, the for-loops with respect to j and k in [Algorithm 4.1](#) can be fully parallelized, making the algorithm well-suited for implementation on parallel computing architectures. The

step size τ in [Algorithm 4.1](#) must satisfy a certain condition (to be specified later) to ensure convergence of the algorithm. Nevertheless, as we will show later, the backtracking line search proposed in [\[57\]](#) can be employed to efficiently determine a suitable step size τ with only marginal additional computational cost at each iteration of [Algorithm 4.1](#).

Remark 4.1. In the linear case, i.e., when $\beta = 0$ in [\(3.2\)](#), [Algorithm 4.1](#) can serve as a preconditioner. In fact, it coincides with the Bramble–Pasciak–Xu preconditioner [\[9\]](#) or the multilevel additive Schwarz preconditioner [\[71, 72\]](#). Convergence analysis of multilevel methods for linear problems posed in $H(\text{div})$ spaces can be found in, e.g., [\[4, 34\]](#).

Remark 4.2. While this paper focuses on parallel multilevel methods (multilevel additive Schwarz), one may also consider successive multilevel methods (multilevel multiplicative Schwarz), such as V-cycle multigrid. These approaches often perform well in practice and may even achieve better convergence rates than parallel methods; see [\[22, Section 4\]](#) and [\[69, Lemma 4.6\]](#). Moreover, they can be parallelized using standard coloring techniques [\[56, Section 5.1\]](#).

However, the analysis of successive subspace correction methods for nearly semi-coercive problems is still lacking. Although the linear case was studied in [\[45\]](#), the analysis relies on the Xu–Zikatanov identity [\[68, 69\]](#), whose extension to convex optimization remains open. For this reason, we leave successive multilevel methods and their analysis for future work.

4.2. Convergence analysis. We present a convergence analysis of the proposed multilevel method in [Algorithm 4.1](#), based on the abstract theory developed in [\[43\]](#). For completeness, a summary of the abstract framework is provided in [section B](#).

Throughout this section, we use the notations $A \lesssim B$ and $B \gtrsim A$ to indicate that there exists a positive constant C , independent of the geometric parameters such as h and J , such that $A \leq CB$. We write $A \approx B$ when both $A \lesssim B$ and $A \gtrsim B$ hold.

First, we observe that the multilevel space decomposition [\(4.1\)](#) satisfies the strengthened convexity condition [\(B.3\)](#) with

$$(4.2) \quad \tau_0 \gtrsim J^{-1} \approx |\log h|^{-1},$$

as a consequence of a coloring argument [\[56, Section 5.1\]](#) applied at each level.

Let F_0 and F_1 be the semicoercive and coercive parts of the energy functional F , respectively, namely,

$$(4.3) \quad F_0(\mathbf{v}) = \frac{1}{2} \int_{\Omega} (\text{div } \mathbf{v} - g_h)^2 dx, \quad F_1(\mathbf{v}) = F(\mathbf{v}) - \int_{\Omega} q_h \text{div } \mathbf{v} dx, \quad \mathbf{v} \in V,$$

so that $F^\epsilon = F_0 + \epsilon F_1$. We define the Bregman divergences associated with F_0 and F_1 by

$$(4.4) \quad \begin{aligned} d_0(\mathbf{w}; \mathbf{v}) &= F_0(\mathbf{v} + \mathbf{w}) - F_0(\mathbf{v}) - \langle F'_0(\mathbf{v}), \mathbf{w} \rangle, \\ d_1(\mathbf{w}; \mathbf{v}) &= F_1(\mathbf{v} + \mathbf{w}) - F_1(\mathbf{v}) - \langle F'_1(\mathbf{v}), \mathbf{w} \rangle, \end{aligned} \quad \mathbf{v}, \mathbf{w} \in V,$$

where $\langle \cdot, \cdot \rangle$ denotes the duality pairing on V . By a direct computation, we observe that

$$(4.5) \quad d_0(\mathbf{w}; \mathbf{v}) = \frac{1}{2} \|\text{div } \mathbf{w}\|_{L^2(\Omega)}^2, \quad \mathbf{v}, \mathbf{w} \in V.$$

Moreover, we have the following lemma concerning d_1 , whose proof is elementary; see, for instance, [\[23\]](#).

LEMMA 4.3. *The Bregman divergence d_1 given in (4.4) satisfies the following:*

- (a) $d_1(\mathbf{w}; \mathbf{v}) \lesssim \|\mathbf{w}\|_{L^2(\Omega)}^2 + (\|\mathbf{v}\|_{L^3(\Omega)} + \|\mathbf{w}\|_{L^3(\Omega)})\|\mathbf{w}\|_{L^3(\Omega)}^2$.
 (b) $d_1(\mathbf{w}; \mathbf{v}) \gtrsim \|\mathbf{w}\|_{L^2(\Omega)}^2 + \|\mathbf{w}\|_{L^3(\Omega)}^3$.

In the abstract convergence theory presented in section B, several assumptions are required to ensure the convergence of subspace correction methods; see Theorem B.5 for the convergence result and Theorems B.1 to B.4 for the corresponding assumptions. In the following, we verify that Algorithm 4.1 satisfies all these assumptions.

The local smoothness condition (Theorem B.1) follows directly from (4.5) and Lemma 4.3(a). The local uniform convexity condition (Theorem B.2) with $p = 3$ is similarly implied by (4.5) and Lemma 4.3(b). Namely, for any bounded and convex subset $K \subset V$, we have

$$(4.6) \quad \mu_{0,K} := \inf_{\mathbf{v}, \mathbf{v}+\mathbf{w} \in K} \frac{d_0(\mathbf{w}; \mathbf{v})}{\|\operatorname{div} \mathbf{w}\|_{L^2(\Omega)}^3} \gtrsim 1, \quad \mu_{1,K} := \inf_{\mathbf{v}, \mathbf{v}+\mathbf{w} \in K} \frac{(d_0 + d_1)(\mathbf{w}; \mathbf{v})}{\|\mathbf{w}\|_X^3} \gtrsim 1.$$

The kernel decomposition condition (Theorem B.3) is satisfied by the patch-based multilevel decomposition (4.1), as discussed in [45, Section 5.1]. Finally, the triangle inequality-like property (Theorem B.4) is a direct consequence of [46, Lemma 5.4]; see also [43, Example C.3].

Given an initial guess $\mathbf{u}^{(0)} \in V$, we define

$$(4.7) \quad K_0 := \{\mathbf{v} \in V : F(\mathbf{v}) \leq F(\mathbf{u}^{(0)})\}.$$

Since all assumptions in Theorem B.5 have been verified, we obtain the following convergence result for Algorithm 4.1 by invoking that theorem.

THEOREM 4.4. *In Algorithm 4.1, assume that $\tau \in (0, \tau_0]$, where τ_0 was given in (4.2). Then there exists $\zeta^* > 0$ such that, if $F^\epsilon(\mathbf{u}^{(0)}) - F^\epsilon(\mathbf{u}_h^\epsilon) > \zeta^*$, then*

$$F^\epsilon(\mathbf{u}^{(1)}) - F^\epsilon(\mathbf{u}_h^\epsilon) \leq \left(1 - \frac{\tau}{2}\right) (F^\epsilon(\mathbf{u}^{(0)}) - F^\epsilon(\mathbf{u}_h^\epsilon)),$$

and otherwise,

$$F^\epsilon(\mathbf{u}^{(n)}) - F^\epsilon(\mathbf{u}_h^\epsilon) \leq \frac{C_1^3}{\tau^3 C_2^2 n^3}, \quad n \geq 1,$$

where C_1 is a positive constant independent of ϵ , except for its implicit dependence on K_0 , and $C_2 = \min\{\mu_{0,K_0}, \mu_{1,K_0}\}$ (see (4.6)).

We note that the convergence theorem above explains how the convergence rate of Algorithm 4.1 depends on the augmented Lagrangian parameter ϵ , but not explicitly on the mesh size h . In fact, the constant C_1 in Theorem 4.4, which is defined in terms of stable decompositions of the multilevel subspaces (4.1) (see [43, Theorem 5.8]), may implicitly depend on h .

While h -independence of multilevel space decompositions for linear problems in $H(\operatorname{div}; \Omega)$ has been established in the literature [4, 34] using the Helmholtz decomposition, extending these arguments to our setting is highly nontrivial. The main difficulty stems from the fact that our problem is posed on the space $X = H(\operatorname{div}; \Omega) \cap L^3(\Omega)^d$, which requires controlling the $L^3(\Omega)^d$ -norm in addition to the $H(\operatorname{div}; \Omega)$ -norm.

In section 5, we provide numerical evidence indicating that the convergence of Algorithm 4.1 is robust with respect to h , similarly to the case of linear problems, across a range of problem settings.

Remark 4.5. Combining [Lemma 4.3\(b\)](#) with the inverse inequality $\|\mathbf{w}\|_{L^3(\Omega)} \lesssim h^{-\frac{d}{6}} \|\mathbf{w}\|_{L^2(\Omega)}$ [[12](#), [Theorem 4.5.11](#)], we can verify that the local uniform convexity condition ([Theorem B.2](#)) holds with $p = 2$, although the constant $\mu_{1,K}$ depends on the mesh size h . Consequently, by invoking [Theorem B.5\(a\)](#), we obtain the linear convergence of [Algorithm 4.1](#). However, the resulting convergence rate is suboptimal due to its dependence on h , which originates from the inverse inequality.

Remark 4.6. In [[58](#)], an alternative approach was proposed for analyzing the ϵ -independence of the convergence rate of subspace correction methods for solving problems of the form (3.2). However, to apply the strategy developed in [[58](#)], one must construct a stable decomposition for the multilevel spaces (4.1) that satisfies certain specific conditions [[58](#), [Assumption 3.1](#)], which is not straightforward.

4.3. Backtracking line search. As stated in [Theorem 4.4](#), the step size τ must be chosen smaller than τ_0 given in (4.2) to guarantee the convergence of [Algorithm 4.1](#). However, in this case, computing an explicit lower bound for τ_0 is needed, and any such estimate may be overly conservative, potentially resulting in slow convergence of [Algorithm 4.1](#). To address this issue, we incorporate a backtracking line search strategy for selecting the step size, as introduced in [[57](#)], into the proposed multilevel method. The resulting algorithm is summarized in [Algorithm 4.2](#).

Algorithm 4.2 Parallel multilevel method for solving (3.2) with backtracking

Choose $\mathbf{u}^{(0)} \in V$ and $\tau^{(0)} > 0$.

for $n = 0, 1, 2, \dots$ **do**

for $j = 1, 2, \dots, J$ **do**

for $k = 1, 2, \dots, n_j$ **do**

$$\mathbf{w}_{j,k}^{(n+1)} = \arg \min_{\mathbf{w}_{j,k} \in V_{j,k}} F^\epsilon(\mathbf{u}^{(n)} + \mathbf{w}_{j,k})$$

end for

end for

$$\tau \leftarrow 2\tau^{(n)}$$

repeat

$$\mathbf{u}^{(n+1)} = \mathbf{u}^{(n)} + \tau \sum_{j=1}^J \sum_{k=1}^{n_j} \mathbf{w}_{j,k}^{(n+1)}$$

$$\mathbf{if} \ F^\epsilon(\mathbf{u}^{(n)}) - F^\epsilon(\mathbf{u}^{(n+1)}) < \tau \sum_{j=1}^J \sum_{k=1}^{n_j} \left(F^\epsilon(\mathbf{u}^{(n)}) - F^\epsilon(\mathbf{u}^{(n)} + \mathbf{w}_{j,k}^{(n+1)}) \right) \ \mathbf{then}$$

$$\tau \leftarrow \frac{\tau}{2}$$

end if

$$\mathbf{until} \ F^\epsilon(\mathbf{u}^{(n)}) - F^\epsilon(\mathbf{u}^{(n+1)}) \geq \tau \sum_{j=1}^J \sum_{k=1}^{n_j} \left(F^\epsilon(\mathbf{u}^{(n)}) - F^\epsilon(\mathbf{u}^{(n)} + \mathbf{w}_{j,k}^{(n+1)}) \right)$$

$$\tau^{(n+1)} = \tau$$

end for

The key idea behind the backtracking strategy is to adaptively select a step size τ such that the global energy decay exceeds the appropriately weighted sum of the local energy decays. From the perspective of computational cost, at the n th outer iteration of [Algorithm 4.2](#), we need to evaluate $F^\epsilon(\mathbf{u}^{(n)})$, $F^\epsilon(\mathbf{u}^{(n)} + \mathbf{w}_{j,k}^{(n+1)})$ for each $1 \leq j \leq J$ and $1 \leq k \leq n_j$, and $F^\epsilon(\mathbf{u}^{(n+1)})$ for different trial values of the step size τ .

Among these quantities, $F^\epsilon(\mathbf{u}^{(n)})$ has already been computed in the previous iteration and can therefore be reused. The values $F^\epsilon(\mathbf{u}^{(n)} + \mathbf{w}_{j,k}^{(n+1)})$ rely on the local updates $\mathbf{w}_{j,k}^{(n+1)}$ and can thus be evaluated locally. Consequently, the only global computation required is the evaluation of $F^\epsilon(\mathbf{u}^{(n+1)})$, which must be repeated for different trial values of τ . However, the number of trials needed to determine $\tau^{(n+1)}$ is typically small when $\tau^{(n)}$ is chosen suitably (cf. [52, Lemma 4]). Hence, the additional computational cost of the backtracking procedure is modest.

It was shown in [57, Lemma 3.1] that the backtracking procedure always terminates, and a lower bound for $\tau^{(n)}$ can be established in terms of τ_0 defined in (4.2). More precisely, from the strengthened convexity condition (B.3), we have

$$\begin{cases} \tau^{(n)} \geq \tau_0 & \text{if } \tau^{(0)} = 2^m \tau_0 \text{ for some } m \in \mathbb{Z}, \\ \tau^{(n)} > \frac{\tau_0}{2} & \text{otherwise.} \end{cases}$$

Therefore, Algorithm 4.2 does not require a priori knowledge of τ_0 .

Moreover, both theoretical and numerical results in [57] demonstrate that the backtracking strategy not only eliminates the need to tune the step size τ but can also improve the convergence rate. The convergence analysis for the backtracking-enhanced method follows similar lines to the case without backtracking; we refer to [57] for details and omit it here.

Remark 4.7. While the backtracking line search introduced here is designed to satisfy the strengthened convexity condition (B.3), enforcing this condition is essential because we use the overlapping space decomposition (4.1). Namely, since updates on the overlap regions are counted multiple times, the step size τ must be chosen sufficiently small so that the total contribution is not too large.

For linear problems, the restricted Schwarz method [18, 26, 28] is a successful approach for handling this multiple-counting issue. Although overlapping decompositions are still used, only the correction supported on the nonoverlapping region is retained, which avoids multiple counting and often improves convergence.

In this sense, restricted Schwarz may serve as an alternative to the backtracking line search. However, the restriction makes the algorithm nonsymmetric, which may complicate the analysis; recent analyses of additive Schwarz methods for convex optimization, such as [43, 56], rely heavily on symmetry.

4.4. Full approximation scheme (FAS). At each iteration of either Algorithms 4.1 and 4.2, we need to solve local problems of the form

$$(4.8) \quad \min_{\mathbf{w}_{j,k} \in V_{j,k}} F^\epsilon(\mathbf{u}^{\text{old}} + \mathbf{w}_{j,k}),$$

where $\mathbf{u}^{\text{old}} \in V$ denotes the current iterate. However, the problem (4.8) requires evaluating the energy F^ϵ on the finest scale at \mathbf{u}^{old} , which may be computationally expensive (cf. [66, Remark 4.2]).

To further reduce the computational cost, we introduce the full approximation scheme (FAS) [10, 11, 13, 20], which replaces (4.8) with an approximate problem that only requires coarse-scale computations on $V_{j,k}$. For completeness, we briefly derive the FAS formulation.

We start from the following variational identity, which follows directly from the optimality condition of (3.2):

$$(4.9) \quad \langle (F^\epsilon)'(\mathbf{u}_h^\epsilon) - (F^\epsilon)'(\mathbf{u}^{\text{old}}), \mathbf{v} \rangle = -\langle (F^\epsilon)'(\mathbf{u}^{\text{old}}), \mathbf{v} \rangle, \quad \mathbf{v} \in V.$$

To reduce the problem (4.9) to one posed on the j th-level subspace V_j with an unknown $\tilde{\mathbf{u}}_j \in V_j$, we replace \mathbf{u}_h^ϵ , \mathbf{u}^{old} , and the test space V in (4.9) by $\tilde{\mathbf{u}}_j$, $\Pi_j \mathbf{u}^{\text{old}}$, and V_j , respectively. Here, $\Pi_j: V \rightarrow V_j$ denotes the canonical interpolation operator [11, 13]. This leads to the following variational problem: find $\tilde{\mathbf{u}}_j \in V_j$ such that

$$(4.10) \quad \langle (F^\epsilon)'(\tilde{\mathbf{u}}_j) - (F^\epsilon)'(\Pi_j \mathbf{u}^{\text{old}}), \mathbf{v}_j \rangle = -\langle (F^\epsilon)'(\mathbf{u}^{\text{old}}), \mathbf{v}_j \rangle, \quad \mathbf{v}_j \in V_j.$$

When solving (4.10) by a patch-based Schwarz method [4, 44], we need to solve the following variational problem defined on $V_{j,k}$: find $\tilde{\mathbf{w}}_{j,k} \in V_{j,k}$ such that

$$(4.11) \quad \langle (F^\epsilon)'(\mathbf{u}^{\text{old}} + \tilde{\mathbf{w}}_{j,k}) - (F^\epsilon)'(\Pi_j \mathbf{u}^{\text{old}}), \mathbf{v}_{j,k} \rangle = -\langle (F^\epsilon)'(\mathbf{u}^{\text{old}}), \mathbf{v}_{j,k} \rangle, \quad \mathbf{v}_{j,k} \in V_{j,k}.$$

Note that (4.11) is equivalent to the following minimization problem:

$$(4.12) \quad \tilde{\mathbf{w}}_{j,k} = \arg \min_{\mathbf{w}_{j,k} \in V_{j,k}} \{ F^\epsilon(\mathbf{u}^{\text{old}} + \mathbf{w}_{j,k}) + \langle (F^\epsilon)'(\mathbf{u}^{\text{old}}) - (F^\epsilon)'(\Pi_j \mathbf{u}^{\text{old}}), \mathbf{w}_{j,k} \rangle \}.$$

Owing to the optimization structure in (4.12), the FAS local problem (4.11) can be interpreted as an inexact local solver in the sense of [43, 56]. A convergence analysis from this perspective is provided in [20].

In summary, Algorithm 4.3 presents a parallel multilevel method for solving (3.2), equipped with both the backtracking line search and the FAS local problem (4.12).

Algorithm 4.3 Parallel multilevel method for solving (3.2) with FAS

Choose $\mathbf{u}^{(0)} \in V$ and $\tau^{(0)} > 0$.

for $n = 0, 1, 2, \dots$ **do**

for $j = 1, 2, \dots, J$ **do**

for $k = 1, 2, \dots, n_j$ **do**

$$\mathbf{w}_{j,k}^{(n+1)} = \arg \min_{\mathbf{w}_{j,k} \in V_{j,k}} \left\{ F^\epsilon(\mathbf{u}^{(n)} + \mathbf{w}_{j,k}) + \langle (F^\epsilon)'(\mathbf{u}^{(n)}) - (F^\epsilon)'(\Pi_j \mathbf{u}^{(n)}), \mathbf{w}_{j,k} \rangle \right\}$$

end for

end for

$\tau \leftarrow 2\tau^{(n)}$

repeat

$$\mathbf{u}^{(n+1)} = \mathbf{u}^{(n)} + \tau \sum_{j=1}^J \sum_{k=1}^{n_j} \mathbf{w}_{j,k}^{(n+1)}$$

if $F^\epsilon(\mathbf{u}^{(n)}) - F^\epsilon(\mathbf{u}^{(n+1)}) < \tau \sum_{j=1}^J \sum_{k=1}^{n_j} \left(F^\epsilon(\mathbf{u}^{(n)}) - F^\epsilon(\mathbf{u}^{(n)} + \mathbf{w}_{j,k}^{(n+1)}) \right)$ **then**

$$\tau \leftarrow \frac{\tau}{2}$$

end if

until $F^\epsilon(\mathbf{u}^{(n)}) - F^\epsilon(\mathbf{u}^{(n+1)}) \geq \tau \sum_{j=1}^J \sum_{k=1}^{n_j} \left(F^\epsilon(\mathbf{u}^{(n)}) - F^\epsilon(\mathbf{u}^{(n)} + \mathbf{w}_{j,k}^{(n+1)}) \right)$

$\tau^{(n+1)} = \tau$

end for

5. Numerical results. In this section, we present numerical results for the proposed multilevel methods (Algorithms 4.1 to 4.3) for solving the Darcy–Forchheimer

model. We also include results for the augmented Lagrangian method ([Algorithm 3.1](#)) to support our theoretical findings. All numerical experiments were conducted using MATLAB R2024b on a desktop equipped with an AMD Ryzen 5 5600X CPU (3.7 GHz, 6 cores), 40 GB RAM, and the Windows 10 Pro operating system.

For the Darcy–Forchheimer model (2.1), we set $\Omega = (0, 1)^2 \subset \mathbb{R}^2$ and assume that $\mathbf{K} = K\mathbf{I}$ for some positive scalar K . Following the settings commonly used in the literature on numerical methods for the Darcy–Forchheimer model, we take $\mu = 1$, $\rho = 1$, and $K = 1$ as in [47, 36, 54], and vary the Forchheimer coefficient $\beta = 0, 10, 20, 30$, as in [36, 47]. Note that the case $\beta = 0$ corresponds to the linear Darcy model.

We consider the following two benchmark examples taken from [54].

Example 5.1. The functions \mathbf{f} and g , and the corresponding exact solutions \mathbf{u} and p of (2.1) are given by

$$\begin{aligned} \mathbf{f}(x, y) &= \left(\frac{\mu}{\rho K} + \frac{\beta}{\rho} e^x \right) (e^x \sin y, e^x \cos y)^T + (y(1-2x)(1-y), x(1-x)(1-2y))^T, \\ g(x, y) &= 0, \quad \mathbf{u}(x, y) = (e^x \sin y, e^x \cos y)^T, \quad p(x, y) = xy(1-x)(1-y). \end{aligned}$$

Example 5.2. The functions \mathbf{f} and g , and the corresponding exact solutions \mathbf{u} and p of (2.1) are given by

$$\begin{aligned} \mathbf{f}(x, y) &= \left(\frac{\mu}{\rho K} + \frac{\beta}{\rho} \sqrt{x^2 e^{2y} + y^2 e^{2x}} \right) (xe^y, ye^x)^T + \pi(\cos \pi x \sin \pi y, \sin \pi x \cos \pi y)^T, \\ g(x, y) &= e^x + e^y, \quad \mathbf{u}(x, y) = (xe^y, ye^x)^T, \quad p(x, y) = \sin \pi x \sin \pi y. \end{aligned}$$

For the finite element discretization of the Darcy–Forchheimer model (2.1), we use the lowest-order rectangular Raviart–Thomas-type conforming mixed finite element space (see (2.3)) defined on a uniform $1/h \times 1/h$ grid, where h denotes the side length of each rectangular element. For the multilevel space decomposition (4.1) of the finite element space, we use the coarsening factor $\gamma = 2^{-1}$ unless stated otherwise. Namely, the number of levels J satisfies $h = 2^{-J}$.

Each local problem in the proposed multilevel methods is solved by the damped Newton method [8], which is known to be globally convergent for convex optimization problems. The stopping criterion is given in terms of the relative energy difference:

$$(5.1) \quad \left| \frac{F_{j,k}^\epsilon(\mathbf{w}_{j,k}^{(n+1)}; \mathbf{u}^{\text{old}}) - F_{j,k}^\epsilon(\mathbf{w}_{j,k}^{(n)}; \mathbf{u}^{\text{old}})}{F_{j,k}^\epsilon(\mathbf{w}_{j,k}^{(n+1)}; \mathbf{u}^{\text{old}})} \right| < 10^{-5},$$

where $\mathbf{w}_{j,k}^{(n)}$ denotes the n th local iterate, \mathbf{u}^{old} denotes the current global iterate, and $F_{j,k}^\epsilon(\cdot; \mathbf{u}^{\text{old}}): V_{j,k} \rightarrow \mathbb{R}$ denotes the corresponding local energy functional.

In all experiments and for all algorithms, we use zero initial guesses. For the nearly semicoercive problem (3.2), we set $q_h = 0$ throughout. In the linear case ($\beta = 0$), we employ [Algorithm 4.1](#) as a preconditioner for the conjugate gradient method [9].

5.1. Augmented Lagrangian method. Numerical results for the augmented Lagrangian method ([Algorithm 3.1](#)) for various values of the augmented Lagrangian parameter ϵ and mesh size h for solving [Theorems 5.1](#) and [5.2](#) are presented in [Tables 0](#) and [1](#), respectively. For the outer iteration, the stopping criterion

$$(5.2) \quad \max \left\{ \frac{\|\mathbf{u}_h^{(n)} - \mathbf{u}_h\|_{\ell^2}}{\|\mathbf{u}_h\|_{\ell^2}}, \frac{\|p_h^{(n)} - p_h\|_{\ell^2}}{\|p_h\|_{\ell^2}} \right\} < 10^{-3},$$

TABLE 1

Number of iterations required by the augmented Lagrangian method ([Algorithm 3.1](#)) to satisfy the stopping criterion (5.2), for various values of the augmented Lagrangian parameter ϵ and mesh size h ([Theorem 5.1](#)).

$\beta = 0$					$\beta = 10$				
$\epsilon \backslash h$	10^0	10^{-1}	10^{-2}	10^{-3}	$\epsilon \backslash h$	10^0	10^{-1}	10^{-2}	10^{-3}
2^{-6}	3	2	1	1	2^{-6}	12	4	2	2
2^{-7}	3	2	1	1	2^{-7}	12	4	2	2
2^{-8}	3	2	1	1	2^{-8}	12	4	2	2
2^{-9}	3	2	1	1	2^{-9}	12	4	2	2

$\beta = 20$					$\beta = 30$				
$\epsilon \backslash h$	10^0	10^{-1}	10^{-2}	10^{-3}	$\epsilon \backslash h$	10^0	10^{-1}	10^{-2}	10^{-3}
2^{-6}	19	5	2	2	2^{-6}	26	6	3	2
2^{-7}	20	5	2	2	2^{-7}	27	6	3	2
2^{-8}	19	5	2	2	2^{-8}	27	6	3	2
2^{-9}	20	5	2	2	2^{-9}	27	6	3	2

TABLE 2

Number of iterations required by the augmented Lagrangian method ([Algorithm 3.1](#)) to satisfy the stopping criterion (5.2), for various values of the augmented Lagrangian parameter ϵ and mesh size h ([Theorem 5.2](#)).

$\beta = 0$					$\beta = 10$				
$\epsilon \backslash h$	10^0	10^{-1}	10^{-2}	10^{-3}	$\epsilon \backslash h$	10^0	10^{-1}	10^{-2}	10^{-3}
2^{-6}	3	2	1	1	2^{-6}	9	3	2	1
2^{-7}	3	2	1	1	2^{-7}	9	3	2	1
2^{-8}	3	2	1	1	2^{-8}	9	3	2	1
2^{-9}	3	2	1	1	2^{-9}	9	3	2	1

$\beta = 20$					$\beta = 30$				
$\epsilon \backslash h$	10^0	10^{-1}	10^{-2}	10^{-3}	$\epsilon \backslash h$	10^0	10^{-1}	10^{-2}	10^{-3}
2^{-6}	15	4	2	2	2^{-6}	20	5	2	2
2^{-7}	15	4	2	2	2^{-7}	20	5	2	2
2^{-8}	15	4	2	2	2^{-8}	20	5	2	2
2^{-9}	15	4	2	2	2^{-9}	20	5	2	2

where $\|\cdot\|_{\ell^2}$ denotes the standard ℓ^2 -norm of the vector of degrees of freedom.

To numerically verify the arbitrarily fast convergence of [Algorithm 3.1](#) stated in [Theorem 3.1](#), we solve each subproblem using a guaranteed solver from the literature. Specifically, each subproblem in [Algorithm 3.1](#) is solved by the damped Newton method [8], with a stopping criterion requiring that the relative energy difference, defined similarly to (5.1), is less than 10^{-5} .

In all cases, we observe that the number of iterations decreases as ϵ decreases, in agreement with [Theorem 3.1](#). Moreover, the number of iterations remains uniformly bounded as the mesh is refined. Hence, we conclude that [Algorithm 3.1](#) converges

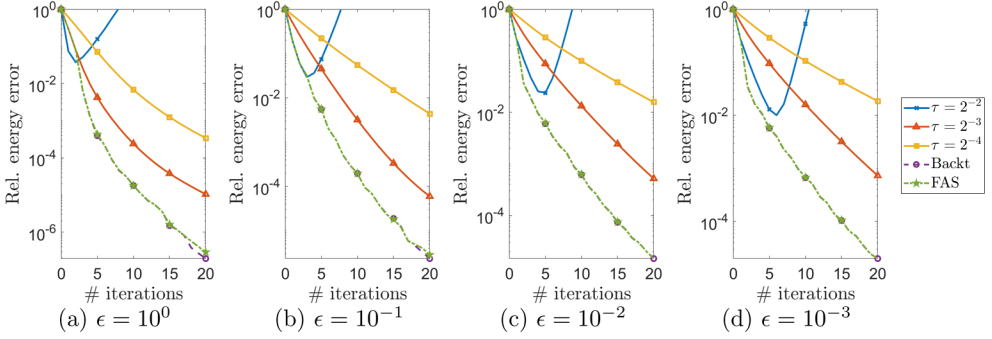


FIG. 2. Convergence curves of the relative energy error $\frac{F^\epsilon(\mathbf{u}^{(n)}) - \min F^\epsilon}{|\min F^\epsilon|}$ for the multilevel method (Algorithm 4.1) with step sizes $\tau = 2^{-2}, 2^{-3}, 2^{-4}$, the backtracking variant (Algorithm 4.2), and the FAS variant (Algorithm 4.3), for various values of the augmented Lagrangian parameter ϵ . Solid, dashed, and dash-dot lines correspond to Algorithms 4.1, 4.2, and 4.3, respectively (Theorem 5.1, $\beta = 30, h = 2^{-8}$).

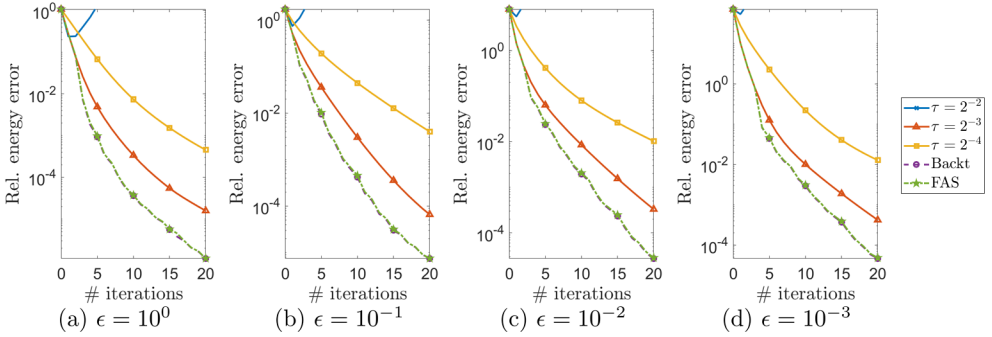


FIG. 3. Convergence curves of the relative energy error $\frac{F^\epsilon(\mathbf{u}^{(n)}) - \min F^\epsilon}{|\min F^\epsilon|}$ for the multilevel method (Algorithm 4.1) with step sizes $\tau = 2^{-2}, 2^{-3}, 2^{-4}$, the backtracking variant (Algorithm 4.2), and the FAS variant (Algorithm 4.3), for various values of the augmented Lagrangian parameter ϵ . Solid, dashed, and dash-dot lines correspond to Algorithms 4.1, 4.2, and 4.3, respectively (Theorem 5.2, $\beta = 30, h = 2^{-8}$).

in very few iterations even for small values of h , provided that ϵ is sufficiently small. These results support our claim that the mixed problem (2.6) can be reduced to the optimization problem (3.2).

5.2. Backtracking line search and FAS. To observe the effects of the backtracking strategy and FAS introduced in Algorithms 4.2 and 4.3, we present convergence curves for the multilevel methods Algorithms 4.1 to 4.3 in Figures 2 and 3, where step sizes $\tau = 2^{-2}, 2^{-3}, 2^{-4}$ are used for Algorithm 4.1. For Algorithm 4.1, we observe that when the step size is set to $\tau = 2^{-2}$, the algorithm diverges in almost all cases, indicating that overly large step sizes may lead to divergence. For smaller step sizes $\tau \leq 2^{-3}$, the algorithm converges in all cases, and larger step sizes among them result in faster convergence. This implies that, provided τ is sufficiently small to ensure convergence, larger values within the admissible range yield better

TABLE 3

Minimum step size $\min_{n \geq 0} \tau^{(n)}$ in the proposed multilevel methods with backtracking (Algorithms 4.2 and 4.3) in the numerical experiments corresponding to Figures 2 and 3.

	$\epsilon = 10^0$	$\epsilon = 10^{-1}$	$\epsilon = 10^{-2}$	$\epsilon = 10^{-3}$
Algorithm 4.2	2^{-3}	2^{-3}	2^{-3}	2^{-3}
Algorithm 4.3	2^{-3}	2^{-3}	2^{-3}	2^{-3}
(a) Theorem 5.1				
	$\epsilon = 10^0$	$\epsilon = 10^{-1}$	$\epsilon = 10^{-2}$	$\epsilon = 10^{-3}$
Algorithm 4.2	2^{-3}	2^{-3}	2^{-4}	2^{-4}
Algorithm 4.3	2^{-3}	2^{-3}	2^{-4}	2^{-4}
(b) Theorem 5.2				

performance.

In contrast, for Algorithm 4.2, which adaptively determines the step size using the backtracking scheme, we consistently observe superior convergence rates across all test cases when compared to Algorithm 4.1. This demonstrates the effectiveness of the backtracking strategy in improving convergence behavior.

Finally, we observe that the convergence curves of Algorithms 4.2 and 4.3 are nearly indistinguishable in all cases. This indicates that using the FAS local solver (4.12) in the proposed multilevel method, as in Algorithm 4.3, does not deteriorate the convergence properties of the algorithm, while significantly reducing the computational cost.

Based on these observations, we focus exclusively on Algorithm 4.3 in the remaining numerical experiments, as it consistently outperforms Algorithm 4.1 in all considered scenarios.

We also report the minimum step sizes $\min_{n \geq 0} \tau^{(n)}$ of Algorithms 4.2 and 4.3 in Table 2. We see that the minimum step size does not decrease significantly even if the augmented Lagrangian parameter ϵ becomes small. This implies that the backtracking scheme is robust with respect to the nearly semicoercive behavior of the problem (3.2).

5.3. Dependence on ϵ , h , and coarsening factor. To assess the robustness and computational efficiency, particularly in parallel settings, of Algorithm 4.3 with respect to the augmented Lagrangian parameter ϵ and the mesh size h , we present numerical results for various values of ϵ and h for Theorems 5.1 and 5.2 in Tables 3 and 4, respectively. The following stopping criterion is used:

$$(5.3) \quad \left| \frac{F^\epsilon(\mathbf{u}^{(n)}) - \min F^\epsilon}{\min F^\epsilon} \right| < 10^{-3}.$$

More precisely, we report:

- Outer iterations: number of outer iterations to satisfy (5.3).
- Local Hessian assembles/solves: number of assemblies and solves of local patch-based Hessian systems (equal for Algorithm 4.3).
- Parallel patch inner solves: ideal parallel cost for solving all local Hessian systems across levels and patches.
- Global reductions: evaluation of $\sum_{j=1}^J \sum_{k=1}^{n_j} \mathbf{w}_{j,k}$ for $\mathbf{w}_{j,k} \in V_{j,k}$.
- Global energy evaluations: evaluation of $F^\epsilon(\mathbf{v})$ for $\mathbf{v} \in V$ (for backtracking).
- Global gradient evaluations: evaluation of $(F^\epsilon)'(\mathbf{v})$ for $\mathbf{v} \in V$.

For the proposed multilevel methods, the numbers of outer iterations, global reduc-

TABLE 4

Numerical results of the proposed multilevel method (Algorithm 4.3, coarsening factor $\gamma = 2^{-1}$) satisfying the stopping criterion (5.3), for various values of the augmented Lagrangian parameter ϵ and mesh size h (Theorem 5.1).

$\beta = 10$													
$\epsilon \backslash h$		outer iterations				local Hessian assembles/solves				parallel patch inner solves			
		10^0	10^{-1}	10^{-2}	10^{-3}	10^0	10^{-1}	10^{-2}	10^{-3}	10^0	10^{-1}	10^{-2}	10^{-3}
2^{-6}		5	9	9	9	1.1E5	1.6E5	1.5E5	1.4E5	41	75	69	69
2^{-7}		5	9	9	9	4.5E5	6.2E5	5.7E5	5.4E5	43	78	72	72
2^{-8}		6	10	10	10	1.8E6	2.4E6	2.2E6	2.1E6	49	90	83	84
2^{-9}		6	10	10	10	6.4E6	8.4E6	8.0E6	7.7E6	53	93	93	87
$\epsilon \backslash h$		global reductions				global energy evaluations				global gradient evaluations			
		10^0	10^{-1}	10^{-2}	10^{-3}	10^0	10^{-1}	10^{-2}	10^{-3}	10^0	10^{-1}	10^{-2}	10^{-3}
2^{-6}		5	9	9	9	11	19	20	19	5	9	9	9
2^{-7}		5	9	9	9	12	19	19	20	5	9	9	9
2^{-8}		6	10	10	10	13	21	21	22	6	10	10	10
2^{-9}		6	10	10	10	14	21	22	23	6	10	10	10

$\beta = 20$													
$\epsilon \backslash h$		outer iterations				local Hessian assembles/solves				parallel patch inner solves			
		10^0	10^{-1}	10^{-2}	10^{-3}	10^0	10^{-1}	10^{-2}	10^{-3}	10^0	10^{-1}	10^{-2}	10^{-3}
2^{-6}		4	8	8	9	8.1E4	1.5E5	1.4E5	1.4E5	34	69	65	70
2^{-7}		5	8	9	9	3.5E5	5.6E5	5.7E5	5.3E5	39	73	76	72
2^{-8}		5	8	10	9	1.3E6	2.0E6	2.1E6	1.9E6	42	73	87	76
2^{-9}		5	9	10	10	5.5E6	7.7E6	7.9E6	7.6E6	43	86	92	90
$\epsilon \backslash h$		global reductions				global energy evaluations				global gradient evaluations			
		10^0	10^{-1}	10^{-2}	10^{-3}	10^0	10^{-1}	10^{-2}	10^{-3}	10^0	10^{-1}	10^{-2}	10^{-3}
2^{-6}		4	8	8	9	9	17	17	19	4	8	8	9
2^{-7}		5	8	9	9	11	18	19	20	5	8	9	9
2^{-8}		5	8	10	9	11	17	22	19	5	8	10	9
2^{-9}		5	9	10	10	11	19	21	21	5	9	10	10

$\beta = 30$													
$\epsilon \backslash h$		outer iterations				local Hessian assembles/solves				parallel patch inner solves			
		10^0	10^{-1}	10^{-2}	10^{-3}	10^0	10^{-1}	10^{-2}	10^{-3}	10^0	10^{-1}	10^{-2}	10^{-3}
2^{-6}		5	7	8	9	1.3E5	1.5E5	1.5E5	1.5E5	48	62	66	72
2^{-7}		5	7	9	9	4.4E5	5.2E5	5.6E5	5.4E5	49	63	75	74
2^{-8}		5	8	9	9	1.5E6	1.9E6	2.0E6	1.9E6	47	73	81	76
2^{-9}		5	8	10	10	5.8E6	6.9E6	7.7E6	7.4E6	47	77	94	89
$\epsilon \backslash h$		global reductions				global energy evaluations				global gradient evaluations			
		10^0	10^{-1}	10^{-2}	10^{-3}	10^0	10^{-1}	10^{-2}	10^{-3}	10^0	10^{-1}	10^{-2}	10^{-3}
2^{-6}		5	7	8	9	11	16	17	19	5	7	8	9
2^{-7}		5	7	9	9	11	15	20	20	5	7	9	9
2^{-8}		5	8	9	9	11	17	19	19	5	8	9	9
2^{-9}		5	8	10	10	12	18	22	21	5	8	10	10

tions, and gradient evaluations coincide, as each is performed once per outer iteration, highlighting communication efficiency. Since the number of Newton iterations varies across local problems, the parallel patch inner solves are defined as the sum of the maximum numbers of inner Newton iterations over all parallel phases, reflecting the per-process cost under full parallelization, while the total number of local Hessian

TABLE 5

Numerical results of the proposed multilevel method ([Algorithm 4.3](#), coarsening factor $\gamma = 2^{-1}$) satisfying the stopping criterion ([5.3](#)), for various values of the augmented Lagrangian parameter ϵ and mesh size h ([Theorem 5.2](#)).

		$\beta = 10$											
$\begin{array}{c} \epsilon \\ h \end{array}$		outer iterations				local Hessian assembles/solves				parallel patch inner solves			
		10^0	10^{-1}	10^{-2}	10^{-3}	10^0	10^{-1}	10^{-2}	10^{-3}	10^0	10^{-1}	10^{-2}	10^{-3}
2^{-6}		6	10	11	11	1.3E5	1.6E5	1.8E5	1.9E5	61	105	117	124
2^{-7}		6	10	12	12	4.5E5	6.0E5	7.0E5	7.7E5	64	113	139	149
2^{-8}		6	11	13	13	1.5E6	2.2E6	2.7E6	2.9E6	65	124	154	170
2^{-9}		7	11	13	14	5.3E6	7.6E6	9.5E6	1.1E7	78	128	153	177
$\begin{array}{c} \epsilon \\ h \end{array}$		global reductions				global energy evaluations				global gradient evaluations			
		10^0	10^{-1}	10^{-2}	10^{-3}	10^0	10^{-1}	10^{-2}	10^{-3}	10^0	10^{-1}	10^{-2}	10^{-3}
2^{-6}		6	10	11	11	13	21	24	23	6	10	11	11
2^{-7}		6	10	12	12	14	22	25	25	6	10	12	12
2^{-8}		6	11	13	13	13	25	27	27	6	11	13	13
2^{-9}		7	11	13	14	15	24	27	30	7	11	13	14

		$\beta = 20$											
$\begin{array}{c} \epsilon \\ h \end{array}$		outer iterations				local Hessian assembles/solves				parallel patch inner solves			
		10^0	10^{-1}	10^{-2}	10^{-3}	10^0	10^{-1}	10^{-2}	10^{-3}	10^0	10^{-1}	10^{-2}	10^{-3}
2^{-6}		5	8	10	11	1.1E5	1.5E5	1.7E5	1.9E5	52	87	112	127
2^{-7}		5	9	11	12	3.9E5	5.7E5	6.7E5	7.6E5	54	104	129	149
2^{-8}		6	10	12	13	1.5E6	2.1E6	2.5E6	2.9E6	65	116	158	171
2^{-9}		6	10	13	14	4.9E6	6.9E6	9.2E6	1.1E7	70	116	158	171
$\begin{array}{c} \epsilon \\ h \end{array}$		global reductions				global energy evaluations				global gradient evaluations			
		10^0	10^{-1}	10^{-2}	10^{-3}	10^0	10^{-1}	10^{-2}	10^{-3}	10^0	10^{-1}	10^{-2}	10^{-3}
2^{-6}		5	8	10	11	11	17	21	23	5	8	10	11
2^{-7}		5	9	11	12	11	19	24	25	5	9	11	12
2^{-8}		6	10	12	13	13	22	25	27	6	10	12	13
2^{-9}		6	10	13	14	13	21	27	30	6	10	13	14

		$\beta = 30$											
$\begin{array}{c} \epsilon \\ h \end{array}$		outer iterations				local Hessian assembles/solves				parallel patch inner solves			
		10^0	10^{-1}	10^{-2}	10^{-3}	10^0	10^{-1}	10^{-2}	10^{-3}	10^0	10^{-1}	10^{-2}	10^{-3}
2^{-6}		5	8	10	11	1.2E5	1.5E5	1.7E5	1.9E5	51	87	110	122
2^{-7}		5	8	11	12	4.1E5	5.3E5	6.6E5	7.6E5	53	93	130	155
2^{-8}		5	9	12	13	1.4E6	2.0E6	2.5E6	2.8E6	56	106	144	164
2^{-9}		5	9	12	14	4.6E6	6.4E6	8.6E6	1.1E7	58	107	145	173
$\begin{array}{c} \epsilon \\ h \end{array}$		global reductions				global energy evaluations				global gradient evaluations			
		10^0	10^{-1}	10^{-2}	10^{-3}	10^0	10^{-1}	10^{-2}	10^{-3}	10^0	10^{-1}	10^{-2}	10^{-3}
2^{-6}		5	8	10	11	11	17	21	23	5	8	10	11
2^{-7}		5	8	11	12	11	18	24	26	5	8	11	12
2^{-8}		5	9	12	13	12	21	25	27	5	9	12	13
2^{-9}		5	9	12	14	11	20	26	29	5	9	12	14

assembles/solves measures the overall computational cost.

We observe that the number of outer iterations does not increase significantly even if either ϵ or h becomes small, which aligns with [Theorem 4.4](#). That is, the performance of [Algorithm 4.3](#) is robust even when the nearly semicoercive behavior of the problem ([3.2](#)) is strong and the scale of the discretized problem is large.

TABLE 6

Numerical results of the proposed multilevel method (Algorithm 4.3, coarsening factor $\gamma = 2^{-2}$) satisfying the stopping criterion (5.3), for various values of the augmented Lagrangian parameter ϵ and mesh size h (Theorem 5.1).

$\beta = 10$

		outer iterations				local Hessian assembles/solves				parallel patch inner solves			
		10^0	10^{-1}	10^{-2}	10^{-3}	10^0	10^{-1}	10^{-2}	10^{-3}	10^0	10^{-1}	10^{-2}	10^{-3}
$h \backslash \epsilon$	2^{-6}	9	15	17	17	1.4E5	2.1E5	2.0E5	1.9E5	69	123	135	132
	2^{-7}	7	13	13	12	4.4E5	6.1E5	5.7E5	5.2E5	56	89	90	81
	2^{-8}	9	15	17	18	1.9E6	2.6E6	2.7E6	2.7E6	77	131	141	145
	2^{-9}	8	13	14	14	6.1E6	7.5E6	7.7E6	7.5E6	66	95	100	96
		global reductions				global energy evaluations				global gradient evaluations			
$h \backslash \epsilon$	10^0	10^0	10^{-1}	10^{-2}	10^{-3}	10^0	10^{-1}	10^{-2}	10^{-3}	10^0	10^{-1}	10^{-2}	10^{-3}
	2^{-6}	9	15	17	17	18	30	35	34	9	15	17	17
	2^{-7}	7	13	13	12	16	27	27	24	7	13	13	12
	2^{-8}	9	15	17	18	18	30	34	36	9	15	17	18
2^{-9}	8	13	14	14	17	26	28	28	8	13	14	14	

$\beta = 20$

		outer iterations				local Hessian assembles/solves				parallel patch inner solves			
		10^0	10^{-1}	10^{-2}	10^{-3}	10^0	10^{-1}	10^{-2}	10^{-3}	10^0	10^{-1}	10^{-2}	10^{-3}
$h \backslash \epsilon$	2^{-6}	7	13	17	17	1.0E5	1.9E5	2.1E5	2.0E5	54	109	135	137
	2^{-7}	6	12	13	12	3.7E5	5.6E5	5.7E5	5.1E5	52	86	92	81
	2^{-8}	8	15	16	17	1.6E6	2.5E6	2.5E6	2.5E6	62	130	135	142
	2^{-9}	7	12	14	14	5.9E6	7.3E6	7.7E6	7.5E6	60	95	105	102
		global reductions				global energy evaluations				global gradient evaluations			
$h \backslash \epsilon$	10^0	10^0	10^{-1}	10^{-2}	10^{-3}	10^0	10^{-1}	10^{-2}	10^{-3}	10^0	10^{-1}	10^{-2}	10^{-3}
	2^{-6}	7	13	17	17	14	27	34	34	7	13	17	17
	2^{-7}	6	12	13	12	12	24	28	24	6	12	13	12
	2^{-8}	8	15	16	17	16	30	34	35	8	15	16	17
2^{-9}	7	12	14	14	15	26	28	29	7	12	14	14	

$\beta = 30$

		outer iterations				local Hessian assembles/solves				parallel patch inner solves			
		10^0	10^{-1}	10^{-2}	10^{-3}	10^0	10^{-1}	10^{-2}	10^{-3}	10^0	10^{-1}	10^{-2}	10^{-3}
$h \backslash \epsilon$	2^{-6}	6	12	16	17	8.8E4	1.8E5	2.1E5	2.0E5	49	98	130	137
	2^{-7}	6	10	13	11	3.7E5	5.1E5	5.7E5	4.8E5	52	76	89	77
	2^{-8}	6	12	16	17	1.3E6	2.2E6	2.5E6	2.5E6	54	104	138	143
	2^{-9}	6	10	13	13	5.1E6	6.1E6	7.0E6	6.8E6	55	82	94	96
		global reductions				global energy evaluations				global gradient evaluations			
$h \backslash \epsilon$	10^0	10^0	10^{-1}	10^{-2}	10^{-3}	10^0	10^{-1}	10^{-2}	10^{-3}	10^0	10^{-1}	10^{-2}	10^{-3}
	2^{-6}	6	12	16	17	13	25	33	35	6	12	16	17
	2^{-7}	6	10	13	11	12	20	26	22	6	10	13	11
	2^{-8}	6	12	16	17	12	24	32	36	6	12	16	17
2^{-9}	6	10	13	13	13	20	27	28	6	10	13	13	

In terms of computational cost, we observe that the number of local Hessian assembles/solves increases by approximately a factor of four when the mesh size h is halved. This indicates that the total computational cost of Algorithm 4.3 scales nearly linearly with the number of degrees of freedom. In contrast, the number of parallel patch inner solves increases only very slowly as the mesh is refined. Thus, under an

TABLE 7

Numerical results of the proposed multilevel method (*Algorithm 4.3*, coarsening factor $\gamma = 2^{-2}$) satisfying the stopping criterion (5.3), for various values of the augmented Lagrangian parameter ϵ and mesh size h (*Theorem 5.2*).

		$\beta = 10$											
		outer iterations				local Hessian assembles/solves				parallel patch inner solves			
$h \backslash \epsilon$		10^0	10^{-1}	10^{-2}	10^{-3}	10^0	10^{-1}	10^{-2}	10^{-3}	10^0	10^{-1}	10^{-2}	10^{-3}
2^{-6}		9	16	19	20	1.4E5	2.2E5	2.6E5	2.9E5	87	161	192	224
2^{-7}		8	11	15	19	4.2E5	5.4E5	7.8E5	1.0E6	79	117	171	236
2^{-8}		10	17	20	21	1.9E6	2.9E6	3.6E6	4.1E6	103	177	218	243
2^{-9}		8	12	15	19	4.9E6	7.2E6	9.9E6	1.4E7	86	134	187	257
		global reductions				global energy evaluations				global gradient evaluations			
$h \backslash \epsilon$		10^0	10^{-1}	10^{-2}	10^{-3}	10^0	10^{-1}	10^{-2}	10^{-3}	10^0	10^{-1}	10^{-2}	10^{-3}
2^{-6}		9	16	19	20	20	32	38	42	9	16	19	20
2^{-7}		8	11	15	19	16	24	30	38	8	11	15	19
2^{-8}		10	17	20	21	20	34	40	43	10	17	20	21
2^{-9}		8	12	15	19	18	24	31	39	8	12	15	19

		$\beta = 20$											
		outer iterations				local Hessian assembles/solves				parallel patch inner solves			
$h \backslash \epsilon$		10^0	10^{-1}	10^{-2}	10^{-3}	10^0	10^{-1}	10^{-2}	10^{-3}	10^0	10^{-1}	10^{-2}	10^{-3}
2^{-6}		7	14	19	19	1.2E5	2.0E5	2.6E5	2.8E5	74	141	195	210
2^{-7}		7	10	14	18	4.0E5	5.0E5	7.1E5	9.8E5	68	102	162	224
2^{-8}		8	14	19	21	1.6E6	2.5E6	3.5E6	4.0E6	85	155	207	234
2^{-9}		7	11	15	18	4.5E6	6.4E6	9.6E6	1.3E7	77	124	186	245
		global reductions				global energy evaluations				global gradient evaluations			
$h \backslash \epsilon$		10^0	10^{-1}	10^{-2}	10^{-3}	10^0	10^{-1}	10^{-2}	10^{-3}	10^0	10^{-1}	10^{-2}	10^{-3}
2^{-6}		7	14	19	19	15	30	38	38	7	14	19	19
2^{-7}		7	10	14	18	14	20	29	36	7	10	14	18
2^{-8}		8	14	19	21	17	28	38	42	8	14	19	21
2^{-9}		7	11	15	18	14	23	30	38	7	11	15	18

		$\beta = 30$											
		outer iterations				local Hessian assembles/solves				parallel patch inner solves			
$h \backslash \epsilon$		10^0	10^{-1}	10^{-2}	10^{-3}	10^0	10^{-1}	10^{-2}	10^{-3}	10^0	10^{-1}	10^{-2}	10^{-3}
2^{-6}		6	13	17	20	1.0E5	1.9E5	2.4E5	2.8E5	58	126	179	214
2^{-7}		6	10	13	17	3.7E5	5.0E5	6.6E5	9.3E5	61	106	149	211
2^{-8}		7	14	18	21	1.4E6	2.5E6	3.3E6	4.0E6	76	153	200	237
2^{-9}		6	10	14	17	4.1E6	5.9E6	9.0E6	1.2E7	67	112	176	232
		global reductions				global energy evaluations				global gradient evaluations			
$h \backslash \epsilon$		10^0	10^{-1}	10^{-2}	10^{-3}	10^0	10^{-1}	10^{-2}	10^{-3}	10^0	10^{-1}	10^{-2}	10^{-3}
2^{-6}		6	13	17	20	12	26	34	41	6	13	17	20
2^{-7}		6	10	13	17	13	21	27	35	6	10	13	17
2^{-8}		7	14	18	21	15	28	36	42	7	14	18	21
2^{-9}		6	10	14	17	12	22	29	34	6	10	14	17

ideal parallel computing environment, the parallel computational cost remains nearly constant even for large-scale problems, highlighting the potential of the proposed multilevel method as a parallel solver.

In terms of communication cost, we observe that the numbers of global reductions and global gradient evaluations coincide with the number of outer iterations, meaning

that communication per iteration is minimal. Moreover, the number of global energy evaluations is only about two to three times the number of outer iterations. This indicates that the backtracking line search requires only a small number of additional energy evaluations per iteration, incurring modest communication overhead while significantly improving the convergence rate, as observed in [Figures 2 and 3](#).

Finally, to examine the effect of the coarsening factor in the multilevel structure, we present in [Tables 5 and 6](#) numerical results for [Algorithm 4.3](#) with coarsening factor $\gamma = 2^{-2}$ in the multilevel space decomposition (4.1). We observe that the number of outer iterations remains robust with respect to the mesh size h , while the robustness with respect to the augmented Lagrangian parameter ϵ deteriorates compared to the case $\gamma = 2^{-1}$, especially for [Theorem 5.2](#); the number of outer iterations increases slightly as ϵ decreases.

Compared with the case $\gamma = 2^{-1}$ in [Tables 3 and 4](#), the number of outer iterations increases. Thus, although fewer parallel subspaces are used, the number of local Hessian assembles/solves, which measures total computational cost, does not improve and may even worsen in some cases. Accordingly, the number of parallel patch inner solves also increases. This indicates that using a smaller coarsening factor does not provide advantages in either serial or parallel computation.

5.4. Comparison with multilevel Newton–Krylov–Schwarz. To assess the nonlinear multilevel decomposition used in the proposed methods, we compare [Algorithm 4.3](#) with the multilevel Newton–Krylov–Schwarz [[14](#), [15](#)] method for solving the nearly semicoercive formulation (3.2), using the same multilevel space decomposition. In the multilevel Newton–Krylov–Schwarz method, the nonlinearity is handled by Newton iterations, and each linearized subproblem involving the global Hessian is solved by a parallel multilevel method. Here, we use the damped Newton method [[8](#)] to ensure global convergence, and each linear subproblem is solved by the preconditioned conjugate gradient method with a standard multilevel additive Schwarz preconditioner [[9](#), [25](#), [71](#), [72](#)]. For the outer Newton iteration, we use the stopping criterion (5.3), as in [Algorithm 4.3](#), while for the inner preconditioned conjugate gradient iterations we require the relative residual to be less than 10^{-5} .

In [Tables 7 and 8](#), we report numerical results for [Algorithm 4.3](#) and the multilevel Newton–Krylov–Schwarz method applied to [Theorems 5.1 and 5.2](#), respectively. For both algorithms, the numbers of outer iterations, as well as the numbers of global energy and gradient evaluations, are comparable. While [Algorithm 4.3](#) does not require assembly of global Hessians, the multilevel Newton–Krylov–Schwarz method requires one global Hessian assembly per outer iteration. On the other hand, [Algorithm 4.3](#) requires about four times more local Hessian assemblies, but each local problem is solved only once, whereas in Newton–Krylov–Schwarz it must be solved multiple times due to the preconditioned conjugate gradient iterations. As a result, the number of local Hessian solves in Newton–Krylov–Schwarz is about ten times larger than in [Algorithm 4.3](#), indicating a significantly higher total computational cost.

For the number of parallel patch inner solves, which measures parallel efficiency, Newton–Krylov–Schwarz requires three to four times more than [Algorithm 4.3](#). Thus, under ideal parallelization, it incurs a proportionally larger computational time. Finally, [Algorithm 4.3](#) requires only one global reduction per outer iteration, whereas Newton–Krylov–Schwarz requires two reductions per inner preconditioned conjugate gradient iteration, leading to substantially higher communication cost. Overall, [Algorithm 4.3](#) is superior in terms of total computational cost, parallel efficiency, and

TABLE 8

Numerical results of the proposed multilevel method (*Algorithm 4.3*, Proposed) and the parallel Newton–Krylov–Schwarz method (NKS) satisfying the stopping criterion (5.3), for various values of mesh size h (*Theorem 5.1*, $\epsilon = 10^{-2}$).

$\beta = 10$								
h	outer iterations		global Hessian assembles		local Hessian assembles		local Hessian solves	
	Proposed	NKS	Proposed	NKS	Proposed	NKS	Proposed	NKS
2^{-6}	9	7	0	7	1.5E5	4.0E4	1.5E5	1.3E6
2^{-7}	9	7	0	7	5.7E5	1.6E5	5.7E5	5.5E6
2^{-8}	10	7	0	7	2.2E6	6.2E5	2.2E6	2.3E7
2^{-9}	10	7	0	7	8.0E6	2.5E6	8.0E6	9.7E7
h	parallel patch inner solves		global reductions		global energy evaluations		global gradient evaluations	
	Proposed	NKS	Proposed	NKS	Proposed	NKS	Proposed	NKS
2^{-6}	69	229	9	229	20	15	9	7
2^{-7}	72	244	9	244	19	15	9	7
2^{-8}	83	261	10	261	21	15	10	7
2^{-9}	93	276	10	276	22	15	10	7

$\beta = 20$								
h	outer iterations		global Hessian assembles		local Hessian assembles		local Hessian solves	
	Proposed	NKS	Proposed	NKS	Proposed	NKS	Proposed	NKS
2^{-6}	8	8	0	8	1.4E5	4.5E4	1.4E5	1.5E6
2^{-7}	9	8	0	8	5.7E5	1.8E5	5.7E5	6.2E6
2^{-8}	10	8	0	8	2.1E6	7.1E5	2.1E6	2.6E7
2^{-9}	10	8	0	8	7.9E6	2.8E6	7.9E6	1.1E8
h	parallel patch inner solves		global reductions		global energy evaluations		global gradient evaluations	
	Proposed	NKS	Proposed	NKS	Proposed	NKS	Proposed	NKS
2^{-6}	65	257	8	257	17	17	8	8
2^{-7}	76	279	9	279	19	17	9	8
2^{-8}	87	295	10	295	22	17	10	8
2^{-9}	92	310	10	310	21	17	10	8

$\beta = 30$								
h	outer iterations		global Hessian assembles		local Hessian assembles		local Hessian solves	
	Proposed	NKS	Proposed	NKS	Proposed	NKS	Proposed	NKS
2^{-6}	8	8	0	8	1.5E5	4.5E4	1.5E5	1.4E6
2^{-7}	9	8	0	8	5.6E5	1.8E5	5.6E5	5.9E6
2^{-8}	9	8	0	8	2.0E6	7.1E5	2.0E6	2.5E7
2^{-9}	10	8	0	8	7.7E6	2.8E6	7.7E6	1.0E8
h	parallel patch inner solves		global reductions		global energy evaluations		global gradient evaluations	
	Proposed	NKS	Proposed	NKS	Proposed	NKS	Proposed	NKS
2^{-6}	66	248	8	248	17	16	8	8
2^{-7}	75	265	9	265	20	16	9	8
2^{-8}	81	283	9	283	19	16	9	8
2^{-9}	94	296	10	296	22	16	10	8

communication efficiency.

Remark 5.3. In *Tables 7* and *8*, we observe that the number of outer iterations of the Newton–Krylov–Schwarz method remains unchanged as the mesh size h is refined in all cases. This phenomenon is consistent with the well-known mesh-independence principle of the Newton method; see, e.g., [2].

6. Conclusion. In this paper, we proposed multilevel methods for solving the Darcy–Forchheimer model based on a nearly semicoercive formulation. We first proved that the Darcy–Forchheimer model, formulated as a mixed problem, can be reduced to a nearly semicoercive convex optimization problem via the augmented Lagrangian method. Then, based on this nearly semicoercive formulation, we developed a multilevel method utilizing multilevel patch-based space decomposition, with convergence analysis demonstrating robustness with respect to the augmented Lagrangian parameter ϵ . Additionally, we introduced a backtracking scheme for line search and an FAS approach for fully localized local problems within the proposed multilevel method.

TABLE 9

Numerical results of the proposed multilevel method (*Algorithm 4.3*, Proposed) and the parallel Newton–Krylov–Schwarz method (NKS) satisfying the stopping criterion (5.3), for various values of mesh size h (*Theorem 5.2*, $\epsilon = 10^{-2}$).

$\beta = 10$								
h	outer iterations		global Hessian assembles		local Hessian assembles		local Hessian solves	
	Proposed	NKS	Proposed	NKS	Proposed	NKS	Proposed	NKS
2^{-6}	11	6	0	6	1.8E5	3.4E4	1.8E5	8.6E5
2^{-7}	12	6	0	6	7.0E5	1.3E5	7.0E5	3.6E6
2^{-8}	13	6	0	6	2.7E6	5.3E5	2.7E6	1.5E7
2^{-9}	13	6	0	6	9.5E6	2.1E6	9.5E6	6.2E7
h	parallel patch inner solves		global reductions		global energy evaluations		global gradient evaluations	
	Proposed	NKS	Proposed	NKS	Proposed	NKS	Proposed	NKS
2^{-6}	117	150	11	150	24	12	11	6
2^{-7}	139	159	12	159	25	12	12	6
2^{-8}	154	168	13	168	27	12	12	6
2^{-9}	153	176	13	176	27	12	13	6

$\beta = 20$								
h	outer iterations		global Hessian assembles		local Hessian assembles		local Hessian solves	
	Proposed	NKS	Proposed	NKS	Proposed	NKS	Proposed	NKS
2^{-6}	10	6	0	6	1.7E5	3.4E4	1.7E5	8.2E5
2^{-7}	11	6	0	6	6.7E5	1.3E5	6.7E5	3.4E6
2^{-8}	12	6	0	6	2.5E6	5.3E5	2.5E6	1.4E7
2^{-9}	13	6	0	6	9.2E6	2.1E6	9.2E6	5.9E7
h	parallel patch inner solves		global reductions		global energy evaluations		global gradient evaluations	
	Proposed	NKS	Proposed	NKS	Proposed	NKS	Proposed	NKS
2^{-6}	112	144	10	144	21	12	10	6
2^{-7}	129	153	11	153	24	12	11	6
2^{-8}	158	160	12	160	25	12	12	6
2^{-9}	158	168	13	168	27	12	13	6

$\beta = 30$								
h	outer iterations		global Hessian assembles		local Hessian assembles		local Hessian solves	
	Proposed	NKS	Proposed	NKS	Proposed	NKS	Proposed	NKS
2^{-6}	10	11	0	11	1.7E5	6.3E4	1.7E5	1.5E6
2^{-7}	11	11	0	11	6.6E5	2.5E5	6.6E5	6.2E6
2^{-8}	12	11	0	11	2.5E6	9.7E5	2.5E6	2.6E7
2^{-9}	12	11	0	11	8.6E6	3.8E6	8.6E6	1.1E8
h	parallel patch inner solves		global reductions		global energy evaluations		global gradient evaluations	
	Proposed	NKS	Proposed	NKS	Proposed	NKS	Proposed	NKS
2^{-6}	110	259	10	259	21	23	10	11
2^{-7}	130	278	11	278	24	23	11	11
2^{-8}	144	292	12	292	25	23	12	11
2^{-9}	145	305	12	305	26	23	12	11

One interesting direction for future research is the rigorous mathematical analysis of the convergence behavior of the proposed multilevel methods with respect to the mesh size h . While h -independent convergence rates of parallel multilevel methods for linear problems have been extensively studied in the literature (e.g., [71, 72]), extending these results to our nonlinear setting poses significant challenges. One major difficulty lies in controlling the $L^3(\Omega)^d$ -norm in addition to the $H(\operatorname{div}; \Omega)$ -norm, as discussed in [section 4](#).

Appendix A. Convergence analysis of the augmented Lagrangian method.

In this appendix, we present a proof of [Theorem 3.1](#) in an abstract setting. That is, we provide a convergence rate analysis of the augmented Lagrangian method [33, 59] for solving convex optimization problems with linear constraints.

Let V and W be finite-dimensional real vector spaces equipped with inner products (\cdot, \cdot) and associated norms $\|\cdot\|$. We consider the following general convex optimization problem with a linear constraint:

$$(A.1) \quad \min_{v \in V} F(v) \quad \text{subject to} \quad Bv = g,$$

where $B: V \rightarrow W$ is a linear operator, $F: V \rightarrow \overline{\mathbb{R}}$ is a convex functional, and $g \in W$. Let $u \in V$ denote a solution to (A.1). The augmented Lagrangian method for solving (A.1) is summarized in Algorithm A.1.

Algorithm A.1 Augmented Lagrangian method for solving (A.1)

Given $\epsilon > 0$:

Choose $p^{(0)} \in W$.

for $n = 0, 1, 2, \dots$ **do**

$$u^{(n+1)} = \arg \min_{v \in V} \left\{ F(v) + (p^{(n)}, Bv - g) + \frac{1}{2\epsilon} \|Bv - g\|^2 \right\}$$

$$p^{(n+1)} = p^{(n)} + \epsilon^{-1} (Bu^{(n+1)} - g)$$

end for

We observe that Algorithm A.1 reduces to Algorithm 3.1 if we set

$$(A.2) \quad V \leftarrow X_h, \quad W \leftarrow M_h, \quad \|\cdot\| \leftarrow \|\cdot\|_{L^2(\Omega)}, \quad F(v) \leftarrow F(v), \quad B \leftarrow -\operatorname{div}, \quad g \leftarrow -g_h.$$

To carry out the convergence analysis, we leverage the equivalence between the augmented Lagrangian method and the proximal point algorithm [48, 62] for solving a dual problem, as established in [37, 61, 65]. By invoking Fenchel–Rockafellar duality [60], the dual problem associated with (A.1) is given by

$$(A.3) \quad \min_{q \in W} \{F^*(-B^*q) + (g, q)\},$$

where $B^*: W \rightarrow V$ denotes the adjoint of B , and $F^*: V \rightarrow \overline{\mathbb{R}}$ is the Legendre–Fenchel conjugate of F , defined by

$$(A.4) \quad F^*(w) = \sup_{v \in V} \{(w, v) - F(v)\}, \quad w \in V.$$

The proximal point algorithm for solving (A.3) is summarized in Algorithm A.2.

Algorithm A.2 Proximal point algorithm for solving (A.3)

Given $\epsilon > 0$:

Choose $q^{(0)} \in W$.

for $n = 0, 1, 2, \dots$ **do**

$$q^{(n+1)} = \arg \min_{q \in W} \left\{ F^*(-B^*q) + (g, q) + \frac{\epsilon}{2} \|q - q^{(n)}\|^2 \right\}$$

end for

In Lemma A.1, we summarize the equivalence between Algorithms A.1 and A.2; see [37, Remark 6.2] for details.

LEMMA A.1. *The augmented Lagrangian method presented in Algorithm A.1 is equivalent to the proximal point algorithm presented in Algorithm A.2 in the following sense: if $p^{(0)} = q^{(0)}$, then we have $p^{(n)} = q^{(n)}$ for all $n \geq 0$.*

Thanks to Lemma A.1, it suffices to analyze Algorithm A.2 in order to establish the convergence rate of Algorithm A.1. In Lemma A.2, we present the convergence result for the proximal point algorithm, as established in [6, Example 23.40]; see also [38, 62].

LEMMA A.2. In (A.3), suppose that $F^* \circ (-B^*)$ is μ -strongly convex for some $\mu > 0$, ensuring that (A.3) admits a unique solution $p \in W$. Then, in the proximal point algorithm presented in Algorithm A.2, we have

$$\|q^{(n+1)} - p\| \leq \frac{\epsilon}{\mu + \epsilon} \|q^{(n)} - p\|, \quad n \geq 0.$$

Remark A.3. For certain convex optimization problems of the form (A.3) arising in partial differential equations (see, e.g., [42]), particularly the dual problem associated with (2.7), the composition $F^* \circ (-B^*)$ is only *locally* strongly convex. Nevertheless, since Algorithm A.2 is a contraction, the sequence $\{q^{(n)}\}$ remains bounded. This boundedness allows the assumption of global strong convexity in Lemma A.2 to be relaxed to a local one. For simplicity and clarity of the analysis, however, we continue to assume global strong convexity throughout. A related discussion appears in [66, Remark 2.1].

Using Lemmas A.1 and A.2, we establish the convergence rate of Algorithm A.1, as stated in Theorem A.4. We remark that Theorem A.4 generalizes [45, Lemma 2.1], which addresses the special case where F is quadratic, i.e., when (A.1) reduces to a linear saddle-point problem.

THEOREM A.4. In (A.3), suppose that $F^* \circ (-B^*)$ is μ -strongly convex. Then, in the augmented Lagrangian method presented in Algorithm A.1, we have

$$(A.5) \quad \|p^{(n+1)} - p\| \leq \frac{\epsilon}{\mu + \epsilon} \|p^{(n)} - p\|, \quad n \geq 0.$$

Moreover, if we further assume that F is differentiable, then we have

$$(A.6) \quad D_F^{\text{sym}}(u^{(n+1)}, u) \leq \begin{cases} \frac{\mu\epsilon^2}{(\mu + \epsilon)^2} \|p^{(n)} - p\|^2, & \text{if } \epsilon \leq \mu, \\ \frac{\epsilon}{4} \|p^{(n)} - p\|^2, & \text{if } \epsilon > \mu, \end{cases} \quad n \geq 0.$$

Proof. The first estimate (A.5) follows immediately from Lemmas A.1 and A.2. To prove (A.6), we first see that the optimality condition for (A.1) reads as

$$(A.7a) \quad \nabla F(u) + B^*p = 0,$$

$$(A.7b) \quad Bu = g.$$

Moreover, Algorithm A.1 reads as

$$(A.8a) \quad \nabla F(u^{(n+1)}) + B^*p^{(n)} + \epsilon^{-1}B^*(Bu^{(n+1)} - g) = 0,$$

$$(A.8b) \quad p^{(n+1)} = p^{(n)} + \epsilon^{-1}(Bu^{(n+1)} - g).$$

Combining (A.7a), (A.7b), and (A.8a) yields

$$(A.9) \quad \nabla F(u^{(n+1)}) - \nabla F(u) + B^*(p^{(n)} - p) + \epsilon^{-1}B^*B(u^{(n+1)} - u) = 0.$$

In addition, combining (A.7b) and (A.8b) yields

$$(A.10) \quad p^{(n+1)} - p^{(n)} = \epsilon^{-1}B(u^{(n+1)} - u).$$

It follows that

$$\begin{aligned}
(A.11) \quad D_F^{\text{sym}}(u^{(n+1)}, u) &\stackrel{(3.1)}{=} (\nabla F(u^{(n+1)}) - \nabla F(u), u^{(n+1)} - u) \\
&\stackrel{(A.9)}{=} -(B^*(p^{(n)} - p), u^{(n+1)} - u) - \epsilon^{-1}(B^*B(u^{(n+1)} - u), u^{(n+1)} - u) \\
&\stackrel{(A.10)}{=} -\epsilon\|p^{(n+1)} - p\|^2 + \epsilon(p^{(n+1)} - p, p^{(n)} - p) \\
&\leq \epsilon \left(\frac{1}{2\theta} - 1 \right) \|p^{(n+1)} - p\|^2 + \frac{\epsilon\theta}{2} \|p^{(n)} - p\|^2,
\end{aligned}$$

where θ is any positive real number. On one hand, if $\epsilon \leq \mu$, setting $\theta = \frac{\epsilon}{\mu + \epsilon} \leq \frac{1}{2}$ in (A.11) yields

$$D_F^{\text{sym}}(u^{(n+1)}, u) \leq \frac{\mu - \epsilon}{2} \|p^{(n+1)} - p\|^2 + \frac{\epsilon^2}{2(\mu + \epsilon)} \|p^{(n)} - p\|^2 \stackrel{(A.5)}{\leq} \frac{\mu\epsilon^2}{(\mu + \epsilon)^2} \|p^{(n)} - p\|^2.$$

On the other hand, if $\epsilon > \mu$, setting $\theta = \frac{1}{2}$ in (A.11) yields

$$D_F^{\text{sym}}(u^{(n+1)}, u) \leq \frac{\epsilon}{4} \|p^{(n)} - p\|^2.$$

This completes the proof. \square

Remark A.5. While the arbitrarily fast convergence of the augmented Lagrangian method stated in [Theorem A.4](#) can be viewed as a direct consequence of classical results [[6](#), [61](#), [62](#)], it has seldom been considered in practice because a very small parameter ϵ typically leads to nearly semicoercive subproblems that are difficult to solve numerically. In a recent work [[43](#)], it was shown that introducing a suitable multilevel structure can mitigate this near-semicoercivity; see [section B](#). Thanks to this result, [Theorem A.4](#) can now be considered in practical settings, as discussed in this paper.

Appendix B. Abstract theory of subspace correction methods for nearly semicoercive problems. In this appendix, we provide a brief summary of the abstract convergence theory of subspace correction methods for nearly semicoercive convex optimization problems, as developed in [[43](#)]. Although the theory in [[43](#)] is formulated in a broader setting, we confine our discussion here to a specific case suitable for our purpose, for the sake of simplicity and clarity.

Let V be a uniformly smooth and uniformly convex Banach space (cf. [[50](#)]) equipped with a norm $\|\cdot\|$ and a continuous seminorm $|\cdot|$. We consider the following nearly semicoercive model problem:

$$(B.1) \quad \min_{v \in V} \{F(v) := F_0(v) + \epsilon F_1(v)\},$$

where $F_0: V \rightarrow \mathbb{R}$ and $F_1: V \rightarrow \mathbb{R}$ are Gâteaux differentiable and convex functionals, and ϵ is a small positive parameter, say $\epsilon \in (0, 1/2]$. We further assume that F_0 is semicoercive with respect to $|\cdot|$ [[43](#), Proposition 2.3], and that F_1 is coercive.

Suppose that the space V admits the following space decomposition:

$$(B.2) \quad V = \sum_{j=1}^J V_j,$$

where each V_j , $1 \leq j \leq J$, is a closed subspace of V . The strengthened convexity condition [43, Equation (3.4)] asserts that there exists a constant $\tau_0 > 0$ such that

$$(B.3) \quad (1 - \tau_0)F(v) + \tau_0 \sum_{j=1}^J F(v + w_j) \geq F \left(v + \tau_0 \sum_{j=1}^J w_j \right), \quad v \in V, w_j \in V_j.$$

The parallel subspace correction method for solving the problem (B.1) based on the space decomposition (B.2) is presented in B.1.

Algorithm B.1 Parallel subspace correction method for solving (B.1)

Given $\tau > 0$:
 Choose $u^{(0)} \in V$.
for $n = 0, 1, 2, \dots$ **do**
 for $j = 1, 2, \dots, J$ **do**
 $w_j^{(n+1)} = \arg \min_{w_j \in V_j} F(u^{(n)} + w_j)$
 end for
 $u^{(n+1)} = u^{(n)} + \tau \sum_{j=1}^J w_j^{(n+1)}$
end for

In the following, we present conditions that should be verified to show convergence of Algorithm B.1. We define the Bregman divergences d_0 and d_1 corresponding to F_0 and F_1 , respectively, as in (4.4). Combination of [43, Proposition 4.9 and Assumption 5.4] yields the following local smoothness condition.

Assumption B.1 (local smoothness). For any $\|\cdot\|$ -bounded and convex subset K of V , we have

$$\sup_{v, v+w \in K} \frac{d_0(w; v)}{\|w\|^2} < \infty \quad \text{and} \quad \sup_{v, v+w \in K} \frac{d_1(w; v)}{\|w\|^2} < \infty.$$

The local uniform convexity condition [43, Assumption 5.9] is presented as follows.

Assumption B.2 (local uniform convexity). For some $p \geq 2$, we have the following:

(a) For any $\|\cdot\|$ -bounded and convex subset K of V , we have

$$\mu_{0,K} := \inf_{v, v+w \in K} \frac{d_0(w; v)}{\|w\|^p} > 0.$$

(b) For any $\|\cdot\|$ -bounded and convex subset K of V , we have

$$\mu_{1,K} := \inf_{v, v+w \in K} \frac{(d_0 + d_1)(w; v)}{\|w\|^p} > 0.$$

Under Theorems B.1 and B.2, we can ensure convergence of Algorithm B.1 [43, Theorem 4.13] (see also [56, Theorem 4.8]). However, in order to ensure ϵ -dependent convergence rate, we need more conditions.

The following kernel decomposition assumption [43, Assumption 5.6], originally introduced in [45] for the analysis of linear problems, plays a critical role in the convergence theory.

Assumption B.3 (kernel decomposition). The kernel $\mathcal{N} = \ker F_0$ of the semicoercive functional F_0 in (B.1) admits the decomposition

$$\mathcal{N} = \sum_{j=1}^J (V_j \cap \mathcal{N}).$$

The next condition, [Theorem B.4](#), describes a triangle-inequality-like property stated in [43, Assumption 5.7].

Assumption B.4 (triangle inequality-like property). For any bounded and convex subset $K \subset V$, there exists a constant $C_K > 0$ such that

$$(B.4) \quad d_1(w + w'; v) \leq C_K (d_1(w; v) + d_1(w'; v)), \quad v \in K, \quad w, w' \in V.$$

Similar to (4.7), given an initial guess $u^{(0)} \in V$ for [Algorithm B.1](#), we define the set K_0 by

$$(B.5) \quad K_0 := \{v \in V : F(v) \leq F(u^{(0)})\}.$$

Note that K_0 depends implicitly on ϵ due to the ϵ -dependence of the energy functional F ; see [43, Remark 5.5]. Under all the assumptions stated above, we obtain the following convergence theorem, which is a direct consequence of [43, Theorems 4.13, 5.8, and 5.10].

THEOREM B.5. *Suppose that [Theorems B.1 to B.4](#) hold. In [Algorithm B.1](#), assume that $\tau \in (0, \tau_0]$, where τ_0 was given in (B.3). Then we have the following:*

(a) *In the case $p = 2$, we have*

$$F(u^{(n)}) - F(u) \leq \left(1 - \frac{\tau}{2} \min \left\{1, \frac{C_2}{C_1}\right\}\right)^n (F(u^{(0)}) - F(u)), \quad n \geq 0,$$

where C_1 is a positive constant independent of ϵ , except for its implicit dependence on K_0 (see (B.5)), and $C_2 = \min\{\mu_{0, K_0}, \mu_{1, K_0}\}$.

(b) *In the case $p > 2$, there exists $\zeta^* > 0$ such that, if $F(u^{(0)}) - F(u) > \zeta^*$, then*

$$F(u^{(1)}) - F(u) \leq \left(1 - \frac{\tau}{2}\right) (F(u^{(0)}) - F(u)),$$

and otherwise,

$$F(u^{(n)}) - F(u) \leq \frac{C_1^{\frac{p}{p-2}}}{\tau^{\frac{p}{p-2}} C_2^{\frac{2}{p-2}} n^{\frac{p}{p-2}}}, \quad n \geq 1,$$

where C_1 and C_2 are as defined in (a).

REFERENCES

- [1] S. ACHARYYA, A. BANERJEE, AND D. BOLEY, *Bregman divergences and triangle inequality*, in Proceedings of the 2013 SIAM International Conference on Data Mining (SDM), Society for Industrial and Applied Mathematics (SIAM), Philadelphia, PA, 2013, pp. 476–484.
- [2] E. L. ALLGOWER, K. BÖHMER, F. POTRA, AND W. RHEINBOLDT, *A mesh-independence principle for operator equations and their discretizations*, SIAM J. Numer. Anal., 23 (1986), pp. 160–169.

- [3] A. C. ARISTOTELOUS, O. KARAKASHIAN, AND S. M. WISE, *A mixed discontinuous Galerkin, convex splitting scheme for a modified Cahn-Hilliard equation and an efficient nonlinear multigrid solver*, *Discrete Contin. Dyn. Syst. Ser. B*, 18 (2013), pp. 2211–2238.
- [4] D. N. ARNOLD, R. S. FALK, AND R. WINTHER, *Multigrid in $H(\text{div})$ and $H(\text{curl})$* , *Numer. Math.*, 85 (2000), pp. 197–217.
- [5] A. ARRARÁS, F. J. GASPAR, L. PORTERO, AND C. RODRIGO, *Geometric multigrid methods for Darcy–Forchheimer flow in fractured porous media*, *Comput. Math. Appl.*, 78 (2019), pp. 3139–3151.
- [6] H. H. BAUSCHKE AND P. L. COMBETTES, *Convex Analysis and Monotone Operator Theory in Hilbert Spaces*, Springer, New York, 2011.
- [7] D. BOFFI, F. BREZZI, AND M. FORTIN, *Mixed Finite Element Methods and Applications*, Springer, Heidelberg, 2013.
- [8] S. BOYD AND L. VANDENBERGHE, *Convex Optimization*, Cambridge University Press, Cambridge, 2004.
- [9] J. H. BRAMBLE, J. E. PASCIAK, AND J. XU, *Parallel multilevel preconditioners*, *Math. Comp.*, 55 (1990), pp. 1–22.
- [10] A. BRANDT, *Multi-level adaptive solutions to boundary-value problems*, *Math. Comp.*, 31 (1977), pp. 333–390.
- [11] A. BRANDT, *Multigrid Techniques: 1984 Guide with Applications to Fluid Dynamics*, Gesellschaft für Mathematik und Datenverarbeitung mbH, St. Augustin, 1984.
- [12] S. C. BRENNER AND L. R. SCOTT, *The Mathematical Theory of Finite Element Methods*, Springer, New York, third ed., 2008.
- [13] E. BUELER AND P. E. FARRELL, *A full approximation scheme multilevel method for nonlinear variational inequalities*, *SIAM J. Sci. Comput.*, 46 (2024), pp. A2421–A2444.
- [14] X.-C. CAI, W. D. GROPP, D. E. KEYES, R. G. MELVIN, AND D. P. YOUNG, *Parallel Newton–Krylov–Schwarz algorithms for the transonic full potential equation*, *SIAM J. Sci. Comput.*, 19 (1998), pp. 246–265.
- [15] X.-C. CAI, W. D. GROPP, D. E. KEYES, AND M. D. TIDRIRI, *Newton–Krylov–Schwarz methods in CFD*, in *Numerical Methods for the Navier–Stokes Equations: Proceedings of the International Workshop Held at Heidelberg, October 25–28, 1993*, Springer, 1994, pp. 17–30.
- [16] X.-C. CAI AND D. E. KEYES, *Nonlinearly preconditioned inexact Newton algorithms*, *SIAM J. Sci. Comput.*, 24 (2002), pp. 183–200.
- [17] X.-C. CAI, D. E. KEYES, AND L. MARCINKOWSKI, *Non-linear additive Schwarz preconditioners and application in computational fluid dynamics*, *Internat. J. Numer. Methods Fluids*, 40 (2002), pp. 1463–1470.
- [18] X.-C. CAI AND M. SARKIS, *A restricted additive Schwarz preconditioner for general sparse linear systems*, *SIAM J. Sci. Comput.*, 21 (1999), pp. 792–797.
- [19] L. CHEN, R. GUO, AND J. WEI, *Transformed primal-dual methods with variable-preconditioners*, arXiv preprint arXiv:2312.12355, (2023).
- [20] L. CHEN, X. HU, AND S. WISE, *Convergence analysis of the fast subspace descent method for convex optimization problems*, *Math. Comp.*, 89 (2020), pp. 2249–2282.
- [21] Z. CHEN, Y. DING, Z. QIN, Y. HE, B. LIANG, Y. QING, Y. XING, AND B. LI, *Effects of high-velocity flow on the temperature field near the wellbore: A review*, in *2023 International Conference on Energy Engineering*, Springer, 2023, pp. 887–912.
- [22] D. CHO, J. XU, AND L. ZIKATANOV, *New estimates for the rate of convergence of the method of subspace corrections*, *Numer. Math. Theory Methods Appl.*, 1 (2008), pp. 44–56.
- [23] P. G. CIARLET, *The Finite Element Method for Elliptic Problems*, Society for Industrial and Applied Mathematics (SIAM), Philadelphia, PA, 2002.
- [24] V. DOLEAN, M. J. GANDER, W. KHERIJ, F. KWOK, AND R. MASSON, *Nonlinear preconditioning: How to use a nonlinear Schwarz method to precondition Newton’s method*, *SIAM J. Sci. Comput.*, 38 (2016), pp. A3357–A3380.
- [25] M. DRYJA, M. V. SARKIS, AND O. B. WIDLUND, *Multilevel Schwarz methods for elliptic problems with discontinuous coefficients in three dimensions*, *Numer. Math.*, 72 (1996), pp. 313–348.
- [26] E. EFSTATHIOU AND M. J. GANDER, *Why restricted additive Schwarz converges faster than additive Schwarz*, *BIT Numer. Math.*, 43 (2003), pp. 945–959.
- [27] F. A. FAIRAG AND J. D. AUDU, *Two-level Galerkin mixed finite element method for Darcy–Forchheimer model in porous media*, *SIAM J. Numer. Anal.*, 58 (2020), pp. 234–253.
- [28] A. FROMMER AND D. B. SZYLD, *An algebraic convergence theory for restricted additive Schwarz methods using weighted max norms*, *SIAM J. Numer. Anal.*, 39 (2001), pp. 463–479.
- [29] A. GAVASKAR, N. GUPTA, B. SASS, R. JANOSY, AND J. HICKS, *Design guidance for application of permeable reactive barriers for groundwater remediation*, tech. report, BATTELLE

- Project Report, 2000.
- [30] V. GIRAULT AND M. F. WHEELER, *Numerical discretization of a Darcy–Forchheimer model*, Numer. Math., 110 (2008), pp. 161–198.
- [31] R. GOEBEL AND R. T. ROCKAFELLAR, *Local strong convexity and local Lipschitz continuity of the gradient of convex functions*, J. Convex Anal., 15 (2008), p. 263.
- [32] S. M. HASSANIZADEH AND W. G. GRAY, *High velocity flow in porous media*, Transp. Porous Media, 2 (1987), pp. 521–531.
- [33] M. R. HESTENES, *Multiplier and gradient methods*, J. Optim. Theory Appl., 4 (1969), pp. 303–320.
- [34] R. HIPTMAIR AND A. TOSELLI, *Overlapping and multilevel Schwarz methods for vector valued elliptic problems in three dimensions*, in Parallel Solution of Partial Differential Equations (Minneapolis, MN, 1997), vol. 120 of IMA Vol. Math. Appl., Springer, New York, 2000, pp. 181–208.
- [35] T. HORNEBER, C. RAUH, AND A. DELGADO, *Fluid dynamic characterisation of porous solids in catalytic fixed-bed reactors*, Micropor. Mesopor. Mat., 154 (2012), pp. 170–174.
- [36] J. HUANG, L. CHEN, AND H. RUI, *Multigrid methods for a mixed finite element method of the Darcy–Forchheimer model*, J. Sci. Comput., 74 (2018), pp. 396–411.
- [37] B. JIANG, J. PARK, AND J. XU, *Connections between convex optimization algorithms and subspace correction methods*, arXiv preprint arXiv:2505.09765, (2025).
- [38] D. KIM, *Accelerated proximal point method for maximally monotone operators*, Math. Program., 190 (2021), pp. 57–87.
- [39] E. L. KUNIANSKY, *Simulating groundwater flow in karst aquifers with distributed parameter models—Comparison of porous-equivalent media and hybrid flow approaches*, tech. report, US Geological Survey, 2016.
- [40] C.-O. LEE AND E.-H. PARK, *A dual iterative substructuring method with a penalty term*, Numer. Math., 112 (2009), pp. 89–113.
- [41] C.-O. LEE AND E.-H. PARK, *A dual iterative substructuring method with a small penalty parameter*, J. Korean Math. Soc., 54 (2017), pp. 461–477.
- [42] Y.-J. LEE AND J. PARK, *On the linear convergence of additive Schwarz methods for the p -Laplacian*, IMA J. Numer. Anal., 45 (2025), pp. 2655–2684.
- [43] Y.-J. LEE AND J. PARK, *Parallel subspace correction methods for semicoercive and nearly semicoercive convex optimization with applications to nonlinear PDEs*, Math. Comp., (2025), <https://doi.org/10.1090/mcom/4172>.
- [44] Y.-J. LEE, J. WU, AND J. CHEN, *Robust multigrid method for the planar linear elasticity problems*, Numer. Math., 113 (2009), pp. 473–496.
- [45] Y.-J. LEE, J. WU, J. XU, AND L. ZIKATANOV, *Robust subspace correction methods for nearly singular systems*, Math. Models Methods Appl. Sci., 17 (2007), pp. 1937–1963.
- [46] W. LIU AND N. YAN, *Quasi-norm local error estimators for p -Laplacian*, SIAM J. Numer. Anal., 39 (2001), pp. 100–127.
- [47] H. LÓPEZ, B. MOLINA, AND J. J. SALAS, *Comparison between different numerical discretizations for a Darcy–Forchheimer model*, Electron. Trans. Numer. Anal., 34 (2009), pp. 187–203.
- [48] B. MARTINET, *Régularisation d'inéquations variationnelles par approximations successives*, Rev. Française Informat. Recherche Opérationnelle, 4 (1970), pp. 154–158.
- [49] G. MEDICI AND L. J. WEST, *Groundwater flow velocities in karst aquifers; importance of spatial observation scale and hydraulic testing for contaminant transport prediction*, Environ. Sci. Pollut. Res. Int., 28 (2021), pp. 43050–43063.
- [50] R. E. MEGGINSON, *An Introduction to Banach Space Theory*, Springer-Verlag, New York, 1998.
- [51] H. MUSTAPHA, L. DE LANGAVANT, AND M. A. GIDDINS, *Darcy and non-Darcy flows in fractured gas reservoirs*, in SPE Reservoir Characterisation and Simulation Conference and Exhibition, SPE, 2015, p. D021S019R001.
- [52] Y. NESTEROV, *Gradient methods for minimizing composite functions*, Math. Program., 140 (2013), pp. 125–161.
- [53] F. NIELSEN AND R. NOCK, *Sided and symmetrized Bregman centroids*, IEEE Trans. Inform. Theory, 55 (2009), pp. 2882–2904.
- [54] H. PAN AND H. RUI, *Mixed element method for two-dimensional Darcy–Forchheimer model*, J. Sci. Comput., 52 (2012), pp. 563–587.
- [55] E.-J. PARK, *Mixed finite element methods for generalized Forchheimer flow in porous media*, Numer. Methods Partial Differential Equations, 21 (2005), pp. 213–228.
- [56] J. PARK, *Additive Schwarz methods for convex optimization as gradient methods*, SIAM J. Numer. Anal., 58 (2020), pp. 1495–1530.
- [57] J. PARK, *Additive Schwarz methods for convex optimization with backtracking*, Comput. Math. Appl., 113 (2022), pp. 332–344.

- [58] J. PARK, *Additive Schwarz methods for semilinear elliptic problems with convex energy functionals: Convergence rate independent of nonlinearity*, SIAM J. Sci. Comput., 46 (2024), pp. A1373–A1396.
- [59] M. J. D. POWELL, *A method for nonlinear constraints in minimization problems*, in Optimization (Sympos., Univ. Keele, Keele, 1968), Academic Press, London-New York, 1969, pp. 283–298.
- [60] R. T. ROCKAFELLAR, *Convex Analysis*, Princeton University Press, Princeton, NJ, 1970.
- [61] R. T. ROCKAFELLAR, *Augmented Lagrangians and applications of the proximal point algorithm in convex programming*, Math. Oper. Res., 1 (1976), pp. 97–116.
- [62] R. T. ROCKAFELLAR, *Monotone operators and the proximal point algorithm*, SIAM J. Control Optim., 14 (1976), pp. 877–898.
- [63] J. J. SALAS, H. LÓPEZ, AND B. MOLINA, *An analysis of a mixed finite element method for a Darcy–Forchheimer model*, Math. Comput. Model., 57 (2013), pp. 2325–2338.
- [64] M. SEDGHI-ASL, E. MORALES-CASIQUE, AND S. M. HASSANIZADEH, *Dispersion in high-porosity porous medium*, J. Porous Media, 26 (2023), pp. 1–12.
- [65] S. SETZER, *Operator splittings, Bregman methods and frame shrinkage in image processing*, Int. J. Comput. Vis., 92 (2011), pp. 265–280.
- [66] X.-C. TAI AND J. XU, *Global and uniform convergence of subspace correction methods for some convex optimization problems*, Math. Comp., 71 (2002), pp. 105–124.
- [67] S. M. WISE, *Unconditionally stable finite difference, nonlinear multigrid simulation of the Cahn–Hilliard–Hele–Shaw system of equations*, J. Sci. Comput., 44 (2010), pp. 38–68.
- [68] J. XU AND L. ZIKATANOV, *The method of alternating projections and the method of subspace corrections in Hilbert space*, J. Amer. Math. Soc., 15 (2002), pp. 573–597.
- [69] J. XU AND L. ZIKATANOV, *Algebraic multigrid methods*, Acta Numer., 26 (2017), pp. 591–721.
- [70] Y. YAO, G. LI, AND P. QIN, *Seepage features of high-velocity non-Darcy flow in highly productive reservoirs*, J. Nat. Gas Sci. Eng., 27 (2015), pp. 1732–1738.
- [71] X. ZHANG, *Multilevel Schwarz methods*, Numer. Math., 63 (1992), pp. 521–539.
- [72] X. ZHANG, *Multilevel Schwarz methods for the biharmonic Dirichlet problem*, SIAM J. Sci. Comput., 15 (1994), pp. 621–644.
- [73] I. ZIÓŁKOWSKA AND D. ZIÓŁKOWSKI, *Fluid flow inside packed beds*, Chem. Eng. Process., 23 (1988), pp. 137–164.